Synthesis and Structure–Affinity Relationships of Spirocyclic Benzopyrans with Exocyclic Amino Moiety

Elisabeth Kronenberg,[†] Frauke Weber,[†] Stefanie Brune,[†] Dirk Schepmann,[†] Carmen Almansa,[‡] Kristina Friedland,[§] Erik Laurini,[∥] Sabrina Pricl,[∥] and Bernhard Wünsch*[,†,⊥]

[†]Institut für Pharmazeutische und Medizinische Chemie der Universität Münster, Corrensstraße 48, D-48149 Münster, Germany

[‡]Esteve Pharmaceuticals S.A., Baldiri Reixach 4-8, 08028 Barcelona, Spain

[§]Pharmakologie und Toxikologie, Institut für Pharmazie und Biochemie, Universität Mainz, Staudinger Weg 5, D-55128 Mainz, Germany

[∥]Molecular Biology and Nanotechnology Laboratory (MolBNL@UniTS), DEA, University of Trieste, 34127 Trieste, Italy

[⊥]Cells-in-motion Cluster of Excellence (EXC 1003-CiM), University of Münster, D-48149 Münster, Germany

Supporting Information

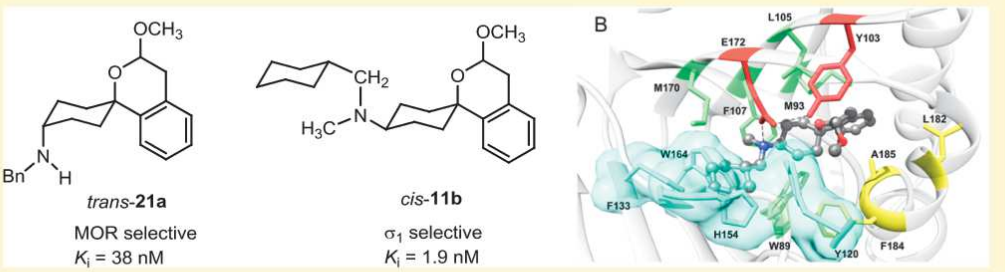

ABSTRACT: σ_1 and/or σ_2 receptors play a crucial role in pathological conditions such as pain, neurodegenerative disorders, and cancer. A set of spirocyclic cyclohexanes with diverse O-heterocycles and amino moieties (general structure **III**) was prepared and pharmacologically evaluated. In structure–activity relationships studies, the σ_1 receptor affinity and σ_1:σ_2 selectivity were correlated with the stereochemistry, the kind and substitution pattern of the O-heterocycle, and the substituents at the exocyclic amino moiety. cis-configured 2-benzopyran *cis*-**11b** bearing a methoxy group and a tertiary cyclohexylmethylamino moiety showed the highest σ_1 affinity (K_i = 1.9 nM) of this series of compounds. In a Ca^{2+} influx assay, *cis*-**11b** behaved as a σ_1 antagonist. *cis*-**11b** reveals high selectivity over σ_2 and opioid receptors. The interactions of the novel σ_1 ligands were analyzed on the molecular level using the recently reported X-ray crystal structure of the σ_1 receptor protein. The protonated amino moiety forms a persistent salt bridge with E172. The spiro[benzopyran-1,1′-cyclohexane] scaffold and the cyclohexylmethyl moiety occupy two hydrophobic pockets. Exchange of the *N*-cyclohexylmethyl moiety by a benzyl group led unexpectedly to potent and selective μ-opioid receptor ligands.

INTRODUCTION

The class of σ receptors[1,2] consists of two subtypes, termed σ_1 and σ_2 receptor. These two subtypes differ in their ligand-binding profile, molecular weight, and their tissue distribution. The σ_1 receptor is a membrane-bound protein which is mainly localized at mitochondria-associated membranes and at the endoplasmic reticulum (ER) in the central nervous system and in peripheral organs like heart and kidney.[3,4] The X-ray crystal structure of the σ_1 receptor has recently been reported by Kruse and coworkers.[5,6] According to this molecular structure, the receptor adopts a unique three-dimensional (3D) topology with a single transmembrane domain. In contrast to all previously proposed 3D models,[7−10] the amino and carboxy termini are located on opposite sides of the membrane. The protein crystallizes as a triangular trimer with one transmembrane helical domain (residues 6−31) at each corner. The cytosolic domain (residues 32−223) is highly structured, and consists of a major β-barrel motif (residues 81−176), flanked by two α-helices (residues 177−223).[5,6]

Regulation of ion channels, modulation of the release and reuptake of neurotransmitters, and participation in intracellular signaling through modulation of Ca^{2+} levels belong to the main functions of the σ_1 receptor.[11−14] It has been reported that the σ_1 receptor plays an important role in several neurological disorders, for example, depression, alcohol, and drug dependence, Parkinson's, Alzheimer's, and Huntington's disease.[14−18] The potential of the σ_1 receptor antagonist S1RA for the treatment of neuropathic pain is currently under investigation in a phase II clinical trial.[19,20] Moreover, the σ_1 receptor expression level is significantly increased in various human tumor cell lines compared to nontumor cells.[21] Though, σ_1 receptors seem to be involved in programmed

cell death (apoptosis), These findings brought σ_1 receptors into focus for the development of antitumor drugs and cancer diagnosis.[22,23]

Until recently, the σ_2 receptor protein was not cloned and its amino acid sequence and structure remained unknown. In 2011, it was postulated that the σ_2 receptor is a part of the progesterone receptor membrane component 1 (PGRMC-1).[24] This hypothesis could not be confirmed, but in 2017, the σ_2 receptor was identified as transmembrane protein 97 (TMEM97), which regulates the sterol transporter in the ER.[25] Because of its overexpression in human tumor cell lines, the σ_2 receptor represents an interesting target for therapy and diagnosis of tumors.[26−28]

In literature, a large number of structurally diverse ligands interacting with the σ_1 receptor are reported. During the last years, spirocyclic piperidines with a rather rigid scaffold emerged as promising σ_1 receptor ligands. High σ_1 receptor affinity was found for spirocyclic 2-benzopyrans of type **I** and **II** with endocyclic amino moiety. In Figure 1 the σ_1 affinity of the corresponding benzyl derivatives is given.[29,30]

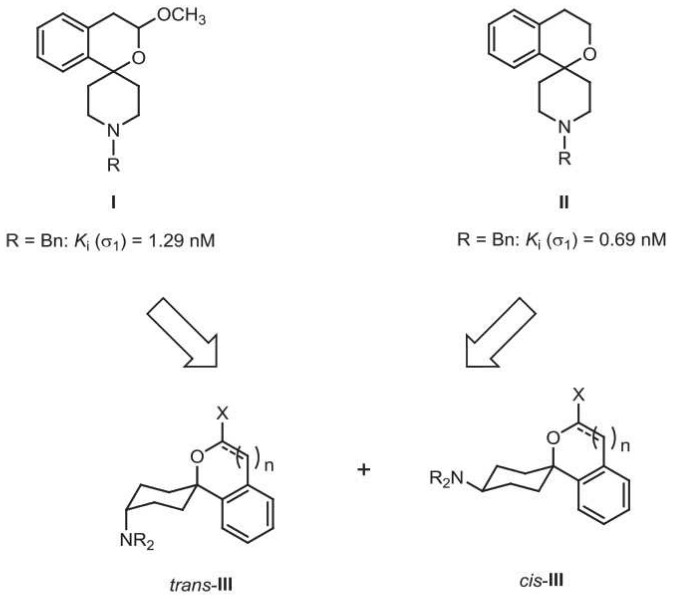

Figure 1. Development of spirocyclic cyclohexanes *trans*-**III** and *cis*-**III** with exocyclic amino moiety derived from spirocyclic piperidine lead compounds **I** and **II** with the endocyclic amino group. The stereodescriptors trans and cis refer to the relative orientation of the O- and N-substituents at the cyclohexane ring.

Based on pharmacophore models, a comprehensive study led to the conclusion that an increased distance between the basic amino moiety and the benzene ring of the spirocyclic framework could be beneficial for high σ_1 receptor affinity. In particular, spirocyclic cyclohexanes of type **III** bearing an exocyclic amino moiety were proposed.[31] In this study, the orientation and substitution pattern of the exocyclic amino moiety and the kind and substituents of the O-heterocycle of **III** should be investigated systematically. Because of the spirocyclic framework, the conformational flexibility of the envisaged ligands of type **III** is rather low, allowing reliable analysis of ligand/receptor interactions. The cyclohexylmethyl and benzyl moieties were the preferred N-substituents considering both secondary and tertiary amines. The synthesis of compound **III** provided two diastereomers termed *trans*- and *cis*-**III**, depending on the relative orientation of O- and N-substituents at the cyclohexane ring.

■ SYNTHESIS

2-Bromobenzaldehyde (**1**) served as starting material for the synthesis of spiro[[2]benzopyran-1,1′-cyclohexan]amines **4**, **5** and **7**, **8**, and **10**, **11** as well as spiro[[2]benzofuran-1,1′-cyclohexan]amines **14** and **15** (Scheme 1). Homologation of aldehyde **1** was performed by a Wittig reaction and subsequent methanol addition.[32] Treatment of dimethyl acetal with *n*-BuLi and subsequently with cyclohexane-1,4-dione yielded the hydroxy acetal **2**.[31] Starting from acetal **2**, intramolecular transacetalization was performed under different reaction conditions to afford the ketones **3**, **6**, and **9**. Treatment of hydroxy acetal **2** with *p*-toluenesulfonic acid in CH_2Cl_2 led to the unsaturated derivative **3**. The ethoxy compound **6** was obtained upon treatment of **2** with *p*-toluenesulfonic acid in $CHCl_3$ stabilized with 1% ethanol, whereas the methoxy derivative **9** resulted from reaction of **2** with catalytic amounts of HCl in CH_2Cl_2.[31] Reductive amination of ketones **3**, **6**, and **9** with cyclohexylmethylamine and $NaBH(OAc)_3$[33] in the presence of one equivalent of acetic acid led to the diastereomeric secondary amines *trans*- and *cis*-**4**, *trans*- and *cis*-**7** and *trans*- and *cis*-**10**, respectively. The secondary amines were obtained in high yields with a slight preference for cis-configured diastereomers with equatorially oriented amino moiety (compare *cis*-**III** in Figure 1). The diastereomeric secondary amines were separated by flash column chromatography and subsequently methylated with formalin and $NaBH(OAc)_3$[33] to afford the tertiary *N*-methyl derivatives *trans*- and *cis*-**5**, *trans*- and *cis*-**8** and *trans*- and *cis*-**11**.

The synthesis of benzofuran derivatives *trans*- and *cis*-**14** and *trans*- and *cis*-**15** started with acetalization of 2-bromobenzaldehyde (**1**) with methanol and trimethyl orthoformate in the presence of *p*-toluenesulfonic acid[18,19] (Scheme 1). Halogen-metal exchange at bromo acetal **12** with *n*-butyllithium and subsequent addition of cyclohexane-1,4-dione followed by intramolecular transacetalization catalyzed by *p*-toluenesulfonic acid led to the spirocyclic ketone **13**. After reductive amination of ketone **13** with cyclohexylmethylamine and $NaBH(OAc)_3$, the secondary amines *trans*- and *cis*-**14** were obtained in 24 and 72% yield, respectively, with a clear preference for the cis-configured diastereomer *cis*-**14**. The predominant formation of cis-configured products resulted from preferred axial attack of the reducing agent, which is explained by stereoelectronic effects. After separation by flash column chromatography both diastereomers were methylated with formalin and $NaBH(OAc)_3$ to afford the tertiary amines *trans*- and *cis*-**15** in high yields.

For the synthesis of saturated 2-benzopyrans **19** and **20** without further substituents in the ring system, 2-(2-bromophenyl)ethanol (**16**) was reacted with PBr_3 to produce the corresponding phenylethyl bromide (Scheme 2). Then, a Parham cyclization[34] was performed upon treatment of the dibromide with *n*-BuLi and, subsequently with monoethylene ketal-protected cyclohexane-1,4-dione. Herein, the aryllithium intermediate reacted with the ketone to form an alcoholate, which cyclized in an intramolecular S_N2 reaction with the ethyl bromide to end up with the 2-benzopyran **17** in 61% yield. Hydrolysis of ethylene ketal **17** with 2 M HCl in Et_2O led to the ketone **18** in 94% yield. Reductive amination of ketone **18** with cyclohexylmethylamine and $NaBH(OAc)_3$

Scheme 1[a]

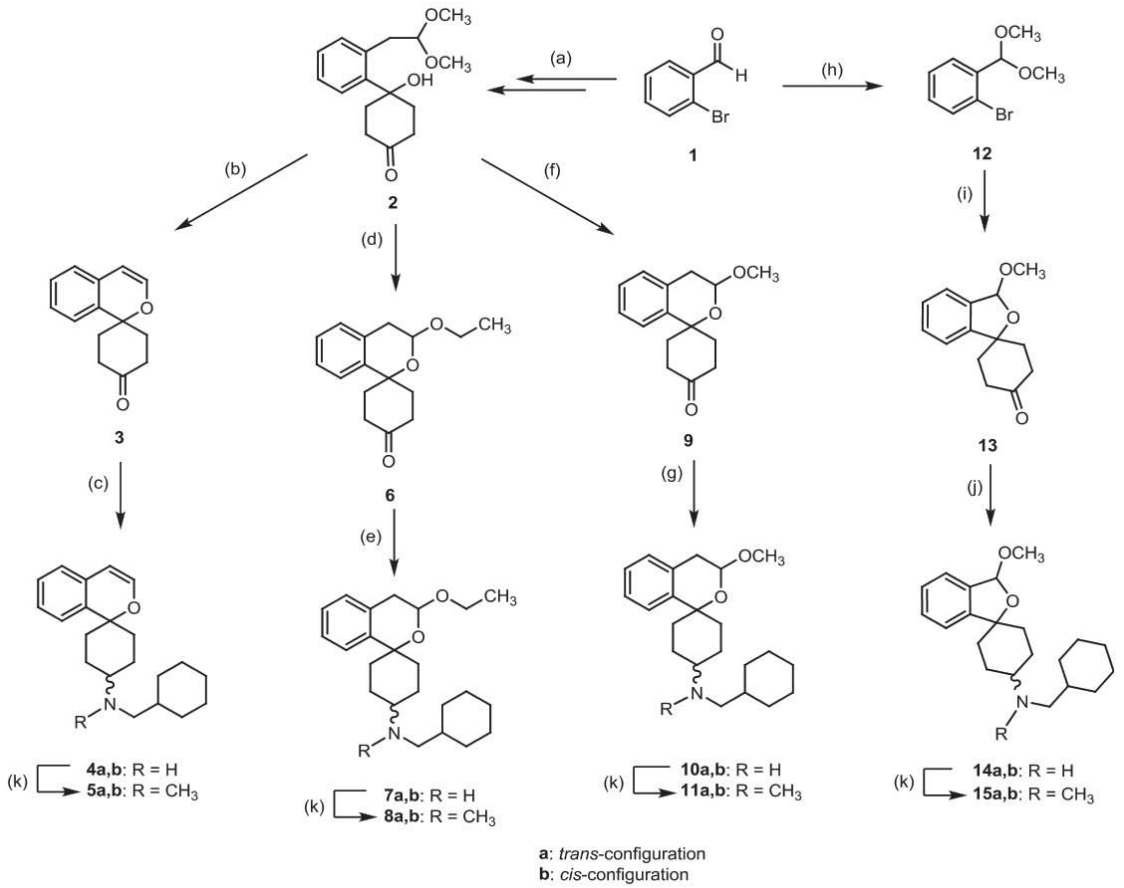

[a]Reagents and reaction conditions: (a) (1) $MeOCH_2PPh_3Cl$, KO^{t}Bu, THF, start at −10 °C, then 16 h at rt, 71%;[32] (2) pTsOH·H_2O, MeOH, 72 h, reflux, 92%;[32] (3) *n*-BuLi, THF, −78 °C, 20 min, then cyclohexane-1,4-dione, 2 h, −78 °C, 1 h, rt, 56%;[31] (b) pTsOH·H_2O, CH_2Cl_2, 6 d, rt, 25%; (c) cyclohexylmethylamine, CH_3CO_2H, $NaBH(OAc)_3$, THF, 3 h, rt, 28% (*trans*-**4a**), 52% (*cis*-**4b**); (d) $CHCl_3$ (stabilized with 1% EtOH), pTsOH·H_2O, 8 d, rt 53%; (e) cyclohexylmethylamine, CH_3CO_2H, $NaBH(OAc)_3$, THF, 3 h, rt, 37% (*trans*-**7a**), 54% (*cis*-**7b**); (f) CH_2Cl_2, HCl, 1,5 h, rt, 81%;[18] (g) cyclohexylmethylamine, CH_3CO_2H, $NaBH(OAc)_3$, THF, 4 h, rt, 37% (*trans*-**10a**), 53% (*cis*-**10b**); (h) pTsOH, CH_3OH, $HC(OCH_3)_3$, 16 h, reflux, 85%;[30] (i) *n*-BuLi, THF, −78 °C, 20 min, then cyclohexane-1,4-dione, 2 h, −78 °C, 1 h, rt; 3. pTsOH·H_2O, THF, rt, 24 h, 44% over two steps; (j) cyclohexylmethylamine, CH_3CO_2H, $NaBH(OAc)_3$, THF, 4 h, rt, 28% (*trans*-**14a**), 67% (*cis*-**14b**); (k) Formalin 37%, $NaBH(OAc)_3$, CH_2Cl_2, 2 h, rt, 81% (*trans*-**5a**), 90% (*cis*-**5b**); 90% (*trans*-**8a**), 92% (*cis*-**8b**); 90% (*trans*-**11a**), 89% (*cis*-**11b**); 99% (*trans*-**15a**), 97% (*cis*-**15b**). Trans ≡ **a**, cis ≡ **b**.

Scheme 2[a]

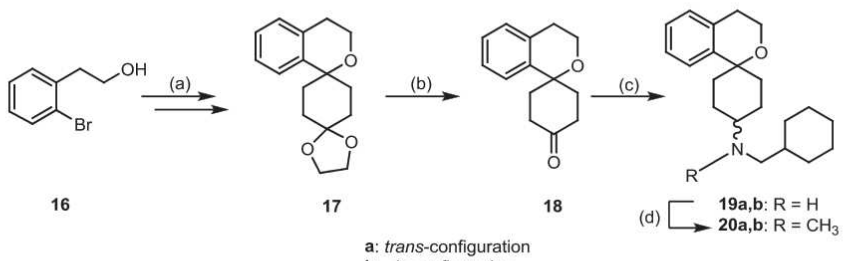

[a]Reagents and reaction conditions: (a) (1) PBr_3, 4 h, 80 °C, 72%; (2) THF, *n*-BuLi, cyclohexane-1,4-dione monoethylene ketal, 5 min, −88 °C, 1 h, rt, 61%; (b) Et_2O, 2 M HCl, 2 d, reflux, 94%; (c) cyclohexylmethylamine, CH_3CO_2H, $NaBH(OAc)_3$, THF, 3 h, rt, 24% (*trans*-**19a**), 72% (*cis*-**19b**); (d) Formalin 37%, $NaBH(OAc)_3$, CH_2Cl_2, 2 h, rt, 97% (*trans*-**20a**), 97% (*cis*-**20b**). trans ≡ **a**, cis ≡ **b**.

generated the trans- and cis-configured secondary amines *trans*-**19a** (24%) and *cis*-**19b** (72%). After separation by flash chromatography (fc), the secondary amines *trans*-**19a** and *cis*-**19b** were methylated with formalin and $NaBH(OAc)_3$ to give the tertiary amines *trans*-**20a** and *cis*-**20b** in high yields.

In order to compare the pharmacological properties of the prepared cyclohexylmethylamines with those of analogous benzylamines, several benzylamines of type **III** were prepared and included into this study (Scheme 3). Thus, ketones **9**, **13**, and **18** were reductively aminated with benzylamine and $NaBH(OAc)_3$[33] to yield three pairs of diastereomeric secondary benzylamines *trans*-**21a**/*cis*-**21b**, *trans*-**23a**/*cis*-**23b**, and *trans*-**24a**/*cis*-**24b**. Exemplarily, the tertiary amines *trans*-**22a** and *cis*-**22b** were prepared by reductive methylation of the secondary amines *trans*-**21a** and *cis*-**21b**, respectively.[31]

Scheme 3[a]

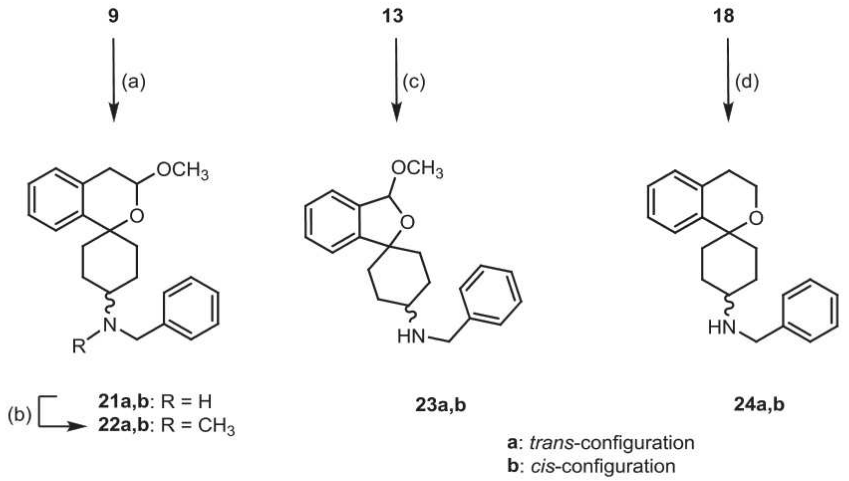

[a]Reagents and reaction conditions: (a) benzylamine, CH_3CO_2H, $NaBH(OAc)_3$, THF, 2 h, rt, 35% (*trans*-**21a**), 52% (*cis*-**21b**);[31] (b) formalin 37%, $NaBH(OAc)_3$, CH_2Cl_2, 3 h, rt, 88% (*trans*-**22a**), 84% (*cis*-**22b**);[31] (c) benzylamine, CH_3CO_2H, $NaBH(OAc)_3$, 4 h, rt, 36% (*trans*-**23a**), 53% (*cis*-**23b**); (d) benzylamine, CH_3CO_2OH, $NaBH(OAc)_3$, 3.5 h, rt, 27% (*trans*-**24a**), 66% (*cis*-**24b**), trans ≡ **a**, cis ≡ **b**

■ σ_1 AND σ_2 RECEPTOR AFFINITY

The σ_1 and σ_2 affinities of all synthesized spirocyclic amines were determined by competition experiments using radioligands. The σ_1 affinity was recorded with homogenates of guinea pig brain and [^{3}H](+)-pentazocine as radioligand. Nonspecific binding was determined with an excess of nonradiolabeled (+)-pentazocine. Rat liver and RT-4 cell membrane preparations served as source for rat (σ_2) and human σ_2 receptors (hσ_2). Because a selective σ_2 radioligand is not available, the nonselective radioligand [^{3}H]di-*o*-tolylguanidine ([^{3}H]DTG) was used in the presence of an excess of (+)-pentazocine to mask the σ_1 receptors.[35−37] Table 1 summarizes the σ_1 and σ_2 affinities of the test compounds together with K_i-values of some reference compounds. Unless otherwise noted, the data represent the mean of three independent experiments (n = 3).

With exception of the tertiary amine **22b** [$K_i(\sigma_1)$ = 24 nM], benzyl-substituted compounds **21**−**24** show lower σ_1 affinity than the corresponding cyclohexylmethyl derivatives. This observation is explained not only by a less effective encasement of the aromatic phenyl moiety but also by an unfavorable conformation of the complete ligand in the binding site (see part "Computer-Assisted Structure−Affinity Relationships").

In general, cis-configured derivatives (**b**-series) reveal higher σ_1 affinity than their trans-configured counterparts (**a**-series). Prominent examples are the pairs of diastereomers *trans*-**4a** (K_i = 12 nM)/*cis*-**4b** (K_i = 5.7 nM) and *trans*-**20a** (K_i = 8.0 nM)/*cis*-**20b** (K_i = 3.1 nM). Only in case of the pairs **14a,b**, **15a,b**, and **19a,b** the affinity of trans- and cis-configured diastereomers is rather similar.

Transformation of the secondary cyclohexylmethylamines **4a,b**, **7a,b**, **10a,b**, **14a,b**, and **19a,b** into methylated tertiary amines led to increased σ_1 receptor affinity. This trend is also found for benzylamines **21a,b**.[31] The ethoxy derivatives **7**/**8** represent nice examples as methylation led to 12-fold and 4-fold increased σ_1 affinity of *trans*-**7a** and *cis*-**7b**, respectively.

Variations of the 2-benzopyran ring of secondary amines has a remarkable impact on σ_1 affinity: compounds **10** with a methoxy moiety in 3-position of the 2-benzopyran system (**10a**: K_i = 19 nM, **10b**: K_i = 5.8 nM) show 5−10-fold higher σ_1 affinity than compounds **7** with an ethoxy moiety (**7a**: K_i = 183 nM, **7b**: K_i = 36 nM). This trend is also observed for the tertiary amines **11** (**11a**: K_i = 3.1 nM, **11b**: K_i = 1.9 nM) and **8** (**8a**: K_i = 15 nM, **8b**: K_i = 8.1 nM). Ligands **4** and **5** with a double bond in 3/4-position and ligands **19** and **20** with a single bond in 3/4-position show almost the same σ_1 affinity as the methoxy derivatives **10** and **11**.

The benzofurans **14** and **15** reveal slightly reduced σ_1 affinity compared to the corresponding benzopyrans **10** and **11**. In the series of benzofurans cis- and trans-configured diastereomers display almost the same σ_1 affinity, but as observed for the benzopyrans methylation increased the σ_1 affinity (**14a**: K_i = 19 nM, **14b**: K_i = 20 nM, **15a**: K_i = 8.0 nM, **15b**: K_i = 8.2 nM).

All test compounds show selectivity or slight preference for the σ_1 over the σ_2 receptor. For most of the compounds the σ_1:σ_2 selectivity is in the range of 5−10. However, particularly high σ_1:σ_2 selectivity was found for trans-configured tertiary amines bearing a cyclohexylmethyl and a methyl moiety at the *N*-atom. Compounds **8a** (σ_1:σ_2 = 24), **11a** (σ_1:σ_2 = 50), **15a** (σ_1:σ_2 = 21), and **20a** (σ_1:σ_2 = 22) represent examples to demonstrate this tendency. Although the cis-configured **b**-analogs (**8b**, **11b**, **15b**, **20b**) reveal higher σ_1 affinity than the corresponding trans-configured **a**-isomers, their σ_1:σ_2 selectivity is lower than the σ_1:σ_2 selectivity of the corresponding trans-configured analogs. This is because of the considerably low σ_2 affinity of trans-configured compounds. Obviously, the σ_2 receptor is more sensitive to the relative configuration of the benzopyrans and benzofurans than the σ_1 receptor: changing the cis-configuration of *cis*-**8b** into trans-configuration (*trans*-**8a**) reduced the σ_1 affinity only 2-fold, but the σ_2 affinity 9-fold resulting in higher σ_1:σ_2 selectivity for *trans*-**8a**.

Within this series of compounds, cis-configured 2-benzopyrans **5b**, **11b**, and **20b** with a tertiary amino moiety (NR_2 = $N(CH_3)CH_2C_6H_{11}$) at the spirocyclic system reveal the highest σ_1 affinity with K_i-values of 2.3, 1.9, and 3.1 nM, respectively. The corresponding trans-configured 2-benzopyrans **5a**, **11a**, and **20a** show lower σ_1 affinity, but higher σ_1:σ_2 selectivity.

Table 1. Receptor Affinities of Spirocyclic 2-Benzopyrans and 2-Benzofurans[d]

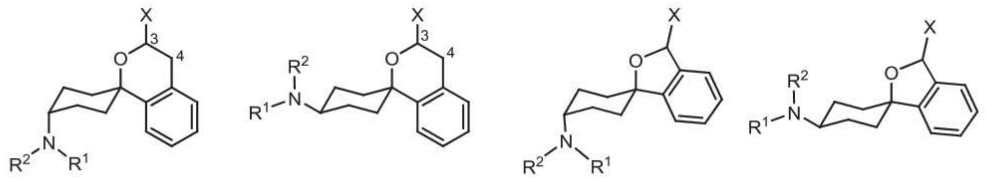

a-series (*trans*) **b**-series (*cis*) **a**-series (*trans*) **b**-series (*cis*)

4, 5, 7, 8, 10, 11, 19, 20, 21, 22, 24 **14, 15, 23**

					K_i ± SEM [nM]					
compd	config	X	R^1	R^2	σ_1	σ_2	hσ_2	MOR	DOR	KOR
4a	trans	C(3)=C(4)	$CH_2C_6H_{11}$	H	12 ± 2.4	53 ± 14	7.0 ± 0.83	258[a]	479[a]	604[a]
4b	cis	C(3)=CC(4)	$CH_2C_6H_{11}$	H	5.7 ± 1.3	67 ± 7.7	6.7 ± 2.7	15%	209[a]	18%
5a	trans	C(3)=CC(4)	$CH_2C_6H_{11}$	CH_3	4.9 ± 0.65	81 ± 13	16 ± 4.1	163[a]	11%	nd
5b	cis	C(3)=CC(4)	$CH_2C_6H_{11}$	CH_3	2.3 ± 0.34	33 ± 3.9	4.6 ± 1.3	391[a]	38%	nd
7a	trans	OEt	$CH_2C_6H_{11}$	H	183 ± 12	161 ± 69	16 ± 4.8	185[a]	185[a]	85
7b	cis	OEt_3	$CH_2C_6H_{11}$	H	36 ± 9.4	308 ± 53	46 ± 2.4	495[a]	432[a]	745[a]
8a	trans	OEt	$CH_2C_6H_{11}$	CH_3	15 ± 1.1	361 ± 51	93 ± 31	879[a]	13%	24%
8b	cis	OEt	$CH_2C_6H_{11}$	CH_3	8.1 ± 1.1	42 ± 4.9	14 ± 1.9	297[a]	356[a]	18%
10a	trans	OCH_3	$CH_2C_6H_{11}$	H	19 ± 4.2	128 ± 28	nd	354 ± 203	228 ± 130	96 ± 44
10b	cis	OCH_3	$CH_2C_6H_{11}$	H	5.8 ± 1.7	101 ± 43	nd	462 ± 297	33%	28%
11a	trans	OCH_3	$CH_2C_6H_{11}$	CH_3	3.1 ± 0.63	154 ± 48	nd	299 ± 48	150 ± 34	980[a]
11b	cis	OCH_3	$CH_2C_6H_{11}$	CH_3	1.9 ± 0.67	12 ± 4.2	13 ± 3.9	391 ± 21	364 ± 62	0%
14a	trans	OCH_3	$CH_2C_6H_{11}$	H	19 ± 3.3	133 ± 30	39 ± 12	273[a]	114[a]	506[a]
14b	cis	OCH_3	$CH_2C_6H_{11}$	H	20 ± 4.9	52 ± 11	11 ± 2.2	501[a]	143[a]	23%
15a	trans	OCH_3	$CH_2C_6H_{11}$	CH_3	8.0 ± 0.47	164 ± 55	9.4 ± 2.2	231[a]	254[a]	639[a]
15b	cis	OCH_3	$CH_2C_6H_{11}$	CH_3	8.2 ± 1.4	70 ± 34	7.6 ± 1.0	16%	559[a]	0%
19a	trans	H	$CH_2C_6H_{11}$	H	15 ± 2.6	99 ± 17	8.0 ± 1.3	114[a]	178[a]	236[a]
19b	cis	H	$CH_2C_6H_{11}$	H	18 ± 3.8	84 ± 19	33 ± 11	841[a]	11%	16%
20a	trans	H	$CH_2C_6H_{11}$	CH_3	8.0 ± 0.71	175 ± 34	12 ± 2.0	nd	187[a]	23%
20b	cis	H	$CH_2C_6H_{11}$	CH_3	3.1 ± 0.32	30 ± 2.5	5.5 ± 2.1	13%	565[a]	10%
21a[31]	trans	OCH_3	Bn	H	538 ± 56	2000[a]	40%	38 ± 13	49 ± 2.7	204 ± 88
21b[31]	cis	OCH_3	Bn	H	158 ± 5.0	[b]	227	20%	41%	27%
22a[31]	trans	OCH_3	Bn	CH_3	43 ± 18	1440[a]	nd	41 ± 18	371[a]	250[a]
22b[31]	cis	OCH_3	Bn	CH_3	24 ± 4.7	329[a]	nd	12%	1300[a]	2300[a]
23a	trans	OCH_3	Bn	H	262[a]	25%[c]	nd	115 ± 51	30%	413[a]
23b	cis	OCH_3	Bn	H	50 ± 4.6	751[a]	nd	768[a]	655[a]	1140[a]
24a	trans	H	Bn	H	256 ± 72	13%[c]	nd	31 ± 11	14 ± 8	85 ± 27
24b	cis	H	Bn	H	97 ± 4.8	503[a]	nd	0%	20%	0%
(+)-pentazocine				5.4 ± 0.5						
DTG				71 ± 8	54 ± 8	20 ± 6				
naloxone							2.1 ± 0.5	2.4 ± 0.5	6.9 ± 0.5	
morphine							3.9 ± 2.1	2.0 ± 0.3	35 ± 6	

[a]Result from one experiment. [b]No correlation between concentration and receptor affinity. [c]Inhibition of radioligand binding at 1 μM concentration of test compound. [d]nd = not determined.

Exemplarily, the affinity of the tertiary amines *trans*-**11a**, *cis*-**11b**, *trans*-**22a**, and *cis*-**22b** toward the human σ_1 receptor was recorded.[38] As for the guinea pig σ_1 receptors the cyclohexylmethylamines *trans*-**11a** [K_i(hσ_1) = 6.9 nM] and *cis*-**11b** [K_i(hσ_1) = 7.3 nM] display higher σ_1 affinity than the corresponding benzylamines *trans*-**22a** [K_i(hσ_1) = 40 nM] and *cis*-**22b** [K_i(hσ_1) = 39 nM]. Although the K_i-values obtained with guinea pig and human σ_1 receptors are not identical, the same trends are observed, which is because of the high-sequence homology (93%)[39] of guinea pig and human σ_1 receptors. It can be concluded that σ_1 receptors from guinea pig can be used as good model for human σ_1 receptors at least for this compound class.

In order to investigate the affinity toward human σ_2 receptors, membrane preparations from RT-4 cells were employed in the same assay as described above. The human urinary bladder cancer cell line RT-4 was used because of its high physiological expression of σ_2 receptors.[40] The K_i-values obtained for most of the test compounds with RT-4-cell membrane preparations are generally 5−10-fold lower than the K_i-values recorded with rat liver membrane preparations. However, in both assay systems the same trends are observed (Table 1).

■ COMPUTER-ASSISTED STRUCTURE−AFFINITY RELATIONSHIP

The experimental affinity values of the present compounds for the σ_1 receptor were rationalized in silico using a combination of docking/free energy-based scoring techniques.[7,41−46] For this purpose, the X-ray crystal structure recently published by Kruse et al. (PDB 5HK1) was used.[5] The computational approach confirmed the structure−affinity relationship deter-

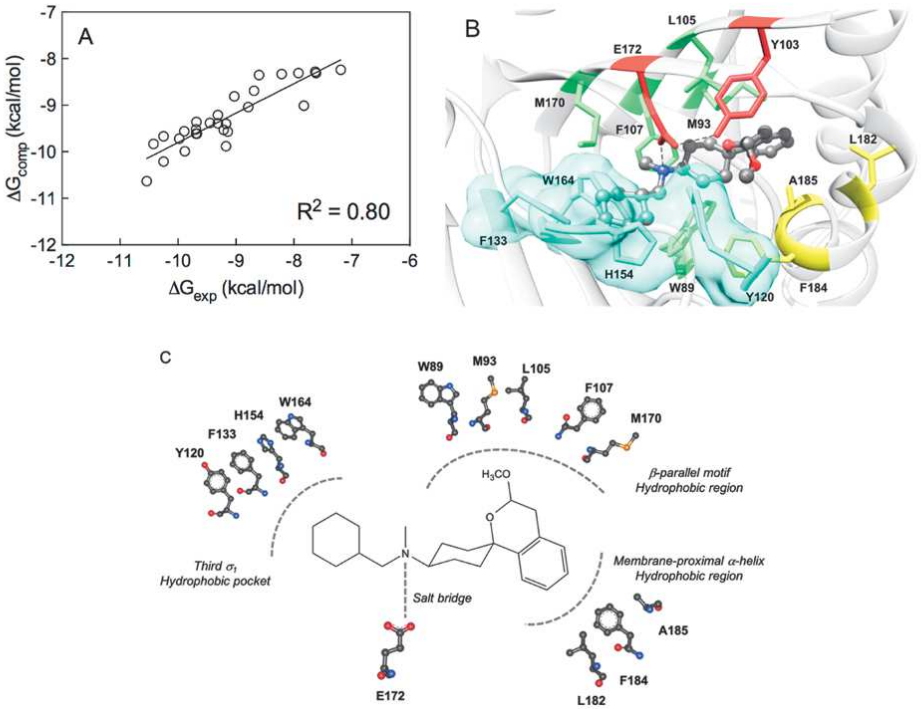

Figure 2. (A) Correlation between the predicted values of the free energy of binding (ΔG_{comp}) for all compounds to the σ_1 receptor (PDB 5HK1) and the corresponding experimental ΔG_{exp}, calculated via the following relationship: $\Delta G_{exp} = -RT \ln(1/K_i(\sigma_1))$ using the $K_i(\sigma_1)$ values listed in Table 1. (B) Compound *cis*-**11b** in complex with the σ_1 receptor (PDB 5HK1). The ligand is shown in atom-colored sticks-and-balls (C, gray; N, blue, O, red); the protein is portrayed as light gray ribbons. The main receptor residues involved in binding *cis*-**11b** are labeled and shown as colored sticks according to the following scheme: E172 and Y103, red; W89, M93, L105, F107, and M170, β-barrel motif, green; L182, F184, and A185, membrane-proximal α-helix, yellow; Y120, F133, H154, and W164, third hydrophobic pocket, cyan with transparent van der Waals surface. Hydrogen atoms, water molecules, ions, and counterions are omitted for clarity. (C) 2D schematic representation of stabilizing interactions between the σ_1 receptor and *cis*-**11b**.

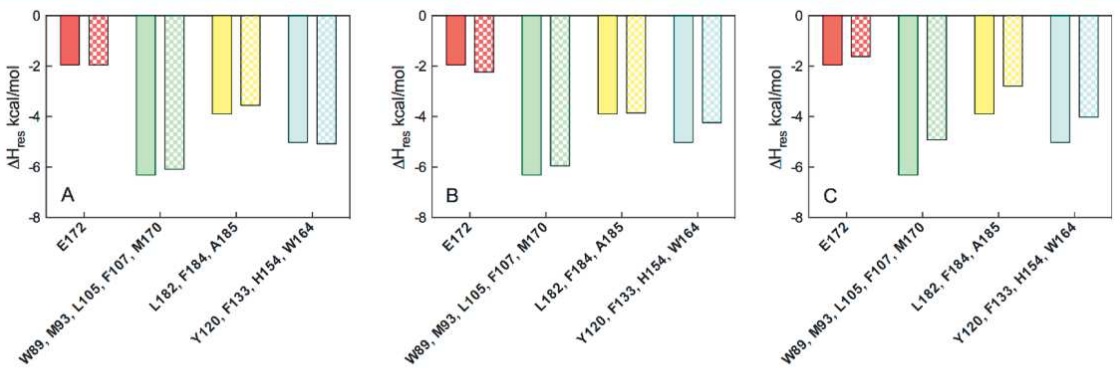

Figure 3. Comparison of the per-residue binding enthalpy decomposition (ΔH_{res}) between the lead compound *cis*-**11b** (solid color bars) and (A) *trans*-**11a**, (B) *cis*-**10b**, and (C) *cis*-**22b** (patterned color bars).

mined by the receptor-binding studies, as testified from the good correlation (R^2 = 0.80) between the calculated free energies of binding and the corresponding experimental values, as shown in Figure 2A (see Table S1 in Supporting Information).

Taking the most potent σ_1 ligand *cis*-**11b** [$K_i(\sigma_1)$ = 1.9 nM] as the reference compound, the analysis of the equilibrated portion of corresponding molecular dynamics (MD) trajectory (Figure 2B) revealed in detail the qualitative pattern of the intermolecular interactions between all these molecules and the σ_1 receptor. Specifically, the basic amine nitrogen of *cis*-**11b** is engaged in a persistent salt bridge with the carboxylate group of E172, this residue being oriented in an optimal position by virtue of an hydrogen bond with Y103 (Figure 2B,C). Two receptor hydrophobic regions concur to nest two lipophilic moieties of *cis*-**11b**: the spiro[cyclohexane-2-benzopyran] group is encased in a cavity lined by the side chains of residues W89, M93, L105, F107, and M170 (belonging to the β-barrel motif) and of residues L182, F184, and A185 of the membrane-proximal α-helix (Figure 2B,C). Finally, the *N*-cyclohexylmethyl moiety of *cis*-**11b** is nicely located within a third hydrophobic pocket made up by residues Y120, F133, H154, and W164 (Figure 2B,C).

The analysis of the binding free energy values ΔG_{comp} coupled with complementary per-residue binding enthalpy decomposition (ΔH_{res}) allowed for further compound/receptor structure−affinity relationship considerations. Taking again the lead compound *cis*-**11b** as a proof-of-concept (ΔG_{comp} = −10.63 ± 0.21 kcal/mol), the saturated benzopyran scaffold appears to be the optimal group for

enhancing the interactions with the σ_1 receptor. Indeed, although no major differences could be identified, both the presence of a double bond as in *cis*-**5b** (ΔG_{comp} = −9.83 ± 0.23 kcal/mol) and a smaller O-heterocycle in the annulated ring system as in the benzofuran derivative *cis*-**15b** (ΔG_{comp} = −9.61 ± 0.18 kcal/mol) led to a decrease in the respective, favorable interactions with the first hydrophobic pocket of the σ_1 binding site.

Other structural modifications deserve a more detailed analysis to justify the experimental/computational affinity results. The prevalent higher affinity of the cis-configured diastereomers with respect to the trans-configured diastereomers can be ascribed to a different orientation of the ligand in the first hydrophobic protein-binding pocket. As an example, Figure 3A shows that the interactions performed by *trans*-**11a** (diastereomer of the reference compound *cis*-**11b**), with the residues W89, M93, L105, F107, and M170 in the β-barrel region, and with amino acids L182, F184, A185 on the proximal transmembrane α-helix provide a lower stabilizing contribution (~0.5 kcal/mol) compared to the lead compound. On the other hand, the salt bridge with E172 and the hydrophobic interactions performed by the cyclohexylmethyl moiety in the third hydrophobic pocket are almost unaffected (Figure 3A).

Methylation of the secondary amine also led to a slight improvement of the σ_1 binding affinity for all test compounds. Although the secondary basic amine of *cis*-**10b** (ΔG_{comp} = −9.99 ± 0.23 kcal/mol) establishes a more favorable salt bridge with E172 compared to *cis*-**11b** (Figure 3B), it fails to establish the same interactions with the second receptor hydrophobic pocket, because of a different orientation of Y120. This, in turn, leads to a slight distortion of that particular region of the receptor. Furthermore, the lack of the methyl group does not provide the optimal interactions with M170 and F107.

Experimentally, the most substantial loss in σ_1 receptor affinity was observed for the series of *N*-benzyl derivatives. In agreement with these in vitro experiments, for these compounds our computational analysis highlights a reduction of about 2 kcal/mol in receptor binding energy. As seen from Figure 3C, compound *cis*-**22b** (ΔG_{comp} = −8.81 ± 0.20 kcal/mol) exhibits lower interaction energies for all amino acids involved in the binding site. This not only implies that the aromatic ring is less effectively encased within the second σ_1 hydrophobic pocket but also that the conformation assumed by the ligand in the receptor binding site is not optimal to guarantee the best interactions with the rest of the involved residues (Figure 3C).

■ σ_1 ANTAGONISTIC ACTIVITY

It has been reported that σ_1 agonists are able to inhibit the KCl-induced Ca^{2+} influx into synaptosomes.[47] Whereas the σ_1 agonist opipramol[48,49] was able to reduce the KCl-induced Ca^{2+} influx, the cyclohexylmethyl derivative *cis*-**11b** [(K_i/σ_1) = 1.9 nM] did not have any effect on the Ca^{2+} influx. In a second experiment, synaptosomes were preincubated with the test compound *cis*-**11b** (10 nM) for 5 min. Then, opipramol (100 μM) was added and after 5 min, the cells were stimulated with KCl (80 mM). Under these conditions, the effect of opipramol on the Ca^{2+} influx was inhibited by the spirocyclic test compound *cis*-**11b**. Both experiments together demonstrate the σ_1 antagonistic effect of *cis*-**11b**.

■ OPIOID RECEPTOR AFFINITY

The affinity of the test compounds toward the opioid receptors μ-opioid receptor (MOR), δ-opioid receptor (DOR) and κ-opioid receptor (KOR) was investigated in receptor-binding studies using radioligands.[50−52] The interaction with opioid receptors was recorded, because the σ receptor was originally considered as one opioid receptor subtype.[1] Moreover, slight variations of potent KOR agonists, for example, amide reduction or change of configuration of the potent KOR agonist U-50488 resulted in potent σ ligands.[53,54] In the class of benzomorphans the configuration defines whether a ligand interacts with σ_1 or opioid receptors.[55,56]

The cyclohexylmethyl-substituted derivatives show low affinity toward all three opioid receptors MOR, DOR, and KOR indicating high selectivity for σ_1 receptors over these opioid receptors.

However, replacement of the cyclohexylmethyl moiety by a benzyl moiety considerably increased the MOR affinity of the ligands. In particular high MOR affinity was found for trans-configured spirocyclic compounds *trans*-**21a−24a** (K_i = 31−115 nM), whereas the corresponding cis-configured analogs *cis*-**21b−24b** show only negligible MOR affinity. Compounds with a benzopyran structure (*trans*-**21a**, *trans*-**22a**, *trans*-**24a**: K_i = 31−41 nM) reveal 3-fold higher MOR affinity than the benzofuran derivative *trans*-**23a**.

Exemplarily, the affinity of *trans*-**22a** toward human MOR was determined in a cell-based assay resulting in a very similar K_i-value of 18 nM instead of 41 nM. The MOR affinity of the trans-configured benzylamines *trans*-**21a−24a** exceeds their σ_1 receptor affinity. Within this series of compounds benzopyrans *trans*-**21a** and *trans*-**24a** with the benzylamino moiety display the highest MOR affinity (K_i = 38 nM, K_i = 31 nM) and MOR:σ_1 selectivity (14-fold, 8.5-fold). It can be concluded that replacement of the cyclohexylmethyl moiety by the benzyl moiety can shift the receptor profile from potent and selective σ_1 receptor ligands toward potent and selective MOR ligands.

The same trend was observed for DOR and KOR affinity, that is, low DOR and KOR affinity was found for cyclohexylmethyl-substituted derivatives, whereas medium to high DOR and KOR affinity was detected for benzylamines. In the small series of benzopyrans higher DOR and KOR affinity was found for trans-configured derivatives *trans*-**21a**, *trans*-**22a**, and *trans*-**24a** than for their *cis*-configured analogs *cis*-**21b**, *cis*-**22b**, and *cis*-**24b**. *trans*-**21a** and *trans*-**24a** showing the highest MOR affinity and MOR:σ_1 selectivity display also the highest DOR (K_i = 49 nM; K_i = 14 nM) and KOR affinity (K_i = 204 nM; K_i = 85 nM). In particular, the DOR affinity of these compounds is in the same range as their MOR affinity.

In Figure 4, the most potent MOR ligand *trans*-**24a** is superposed with the potent MOR activating analgesic fentanyl. It can be seen that the phenylethylpiperidine substructure of fentanyl adopts the same orientation as the benzylaminocyclohexane substructure of *trans*-**24a**. The phenyl ring of fentanyl and the benzopyran structure of *trans*-**24a** have the same position in both compounds. Finally, the propionamide and the pyran ring are regarded as equivalent.

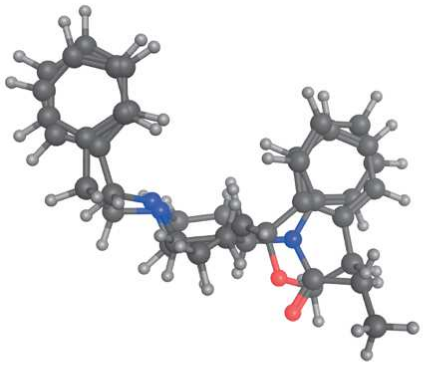

Figure 4. Superposition of *trans*-**24a** with fentanyl. After stochastic conformational analysis, a flexible alignment of *trans*-**24a** and fentanyl was performed. Only reliable, energetically favored conformations (small ΔU values) were considered in the alignment.

SELECTIVITY OVER FURTHER RECEPTORS

The affinity of some ligands toward the phencyclidine (PCP) binding site of the NMDA receptor was recorded exemplarily. Binding at the PCP binding site was considered because small variations of σ_1 ligands can lead to strong interactions with the PCP binding site. In the class of benzomorphans, dextrorotatory enantiomers show high affinity toward σ_1 receptors, whereas laevorotatory enantiomers display high PCP affinity.[55−57] In the binding assay with the radioligand [^{3}H](+)-MK-801,[57,58] the secondary and tertiary cyclohexylmethylamines *trans*-**10a**, *cis*-**10b**, and *trans*-**11a**, *cis*-**11b**, as well as the secondary and tertiary benzylamines *trans*-**21a**, *cis*-**21b**, and *trans*-**22a**, *cis*-**22b** did not show any interaction with the PCP binding site of the NMDA receptor up to a concentration of 1 μM. These results led to the conclusion that the spirocyclic compounds display high selectivity for the σ_1 receptor over the PCP binding site of the NMDA receptor.

The promising diastereomeric tertiary amines *trans*-**11a** [$K_i(\sigma_1)$ = 3.1 nM] and *cis*-**11b** [$K_i(\sigma_1)$ = 1.9 nM] with an *N*-cyclohexylmethyl moiety and *trans*-**22a** [$K_i(\sigma_1)$ = 43 nM; K_i(MOR) = 41 nM] and *cis*-**22b** [$K_i(\sigma_1)$ = 24 nM; K_i(MOR) > 1 μM] with an *N*-benzyl moiety were selected for a small receptor screening. The compounds were tested at a concentration of 1 μM for their interaction with various transporters and receptors.[59] At this ligand concentration, the test compounds did not interact with noradrenalin, dopamine, and serotonin transporters as well as with α_{1A}, α_{2A}, 5-HT$_{1A}$, and 5-HT$_{2B}$ receptors. The only exception was the most potent σ_1 receptor ligand *cis*-**11b** displaying moderate affinity at a concentration of 1 μM toward α_{1A} (68%), α_{2A} (93%), 5-HT$_{1A}$ (60%), and 5-HT$_{2B}$ (62%) receptors. Up to the rather high concentration of 100 μM cytotoxicity of the four compounds was not observed.

PHARMACOKINETIC STUDIES

In order to analyze, whether the compound class is appropriate for in vivo evaluation in neuropathic pain (σ_1 ligands) or general pain (MOR ligands) mouse models, preliminary physicochemical, and pharmacokinetic studies were performed with the diastereomeric tertiary cyclohexylmethylamines *trans*-**11a** and *cis*-**11b** and tertiary benzylamines *trans*-**22a** and *cis*-**22b**. The calculated log *P* values of the cyclohexylmethylamines **11** (clog *P* = 4.9) is higher by 0.6 units than the clog *P* value of the corresponding benzylamines **22** (clog *P* = 4.3).

In a screening, the four test compounds did not inhibit the CYP enzymes CYP1A2, CYP2C9, CYP2C19, and CYP3A4.[60] In particular, the missing interaction with important CYP3A4 should be emphasized. However, all four compounds showed more than 90% inhibition of CYP2D6. In case of further development, CYP2D6 inhibition has to be carefully observed.

In order to get an idea about the metabolic stability, the four test compounds were incubated with human liver microsomes and NADPH. After 60 min, more than 50% of the parent compounds remained intact indicating promising metabolic stability.

CONCLUSIONS

Compared to the spirocyclic piperidines **I** and **II** the distance between the basic amino moiety and the benzene ring and the relative orientation of the amino group and its substituents are modified in the newly designed spirocyclic compounds of type **III**. Although the orientation is modified, the 3D arrangement of the various functional groups is well defined. Moreover, the spirocyclic cyclohexanes allow a broader modification of the basic amino moiety by introduction of two substituents.

A set of 28 spirocyclic amines was synthesized in multistep syntheses. Secondary cyclohexylmethylamines reveal high σ_1 receptor affinity, but tertiary, *N*-methylated analogues display even higher σ_1 affinity. cis-Configured diastereomers show higher σ_1 affinity than their trans-configured counterparts. Variation of the 2-benzopyran ring does not affect the σ_1 receptor affinity considerably. Exemplarily, the σ_1 receptor antagonistic activity of tertiary cyclohexylmethylamine *cis*-**11b** (K_i = 1.9 nM) was confirmed in a Ca^{2+} influx assay. MDs calculations based on the recently published X-ray crystal structure of the σ_1 receptor led to a nice correlation between the recorded affinity (K_i-values transformed into ΔG_{exp}) and the predicted free energy of binding (ΔG_{comp}) for all compounds. The spirocyclic ligands adopt similar binding poses in the binding pocket with a permanent ionic interaction between the protonated amino moiety and the carboxylate moiety of E172 as crucial interaction. The lipophilic parts of the ligands, that is, the spiro[benzopyran-1,1′-cyclohexane] and the cyclohexylmethyl moieties are encased in two lipophilic pockets of the receptor protein.

Unexpectedly, changing the *N*-cyclohexylmethyl into an *N*-benzyl moiety led to a dramatic change of the receptor profile. Whereas the *N*-cyclohexylmethyl derivatives reveal only low MOR, DOR, and KOR affinity, the analogous *N*-benzyl derivatives show high MOR affinity. Because the MOR affinity resides predominantly in the trans-configured diastereomers displaying lower σ_1 affinity, the MOR:σ_1 selectivity is rather high, for example, for *trans*-**21a** (14-fold) and *trans*-**24a** (8-fold). In summary, cis-configured spiro[benzopyran-1.1′-cyclohexanes] bearing a cyclohexylmethyl moiety represent high-affinity and selective σ_1 ligands (e.g., *cis*-**10b**, *cis*-**19b**), whereas the corresponding trans-configured analogs *trans*-**21a** and *trans*-**24a** with an *N*-benzyl group interact with remarkable affinity and selectivity with MOR. These results demonstrate nicely that small changes of the substituents (e.g., $C_5H_{11}CH_2$ into $C_6H_5CH_2$) and the stereochemistry (cis-into trans-configuration) could lead to dramatic changes in the affinity profile of compounds.

EXPERIMENTAL SECTION

Chemistry, General. Thin-layer chromatography: silica gel 60 F254 plates (Merck) were used. fc: silica gel 60, 40−43 μm (Merck)

was used; parentheses include: diameter of the column, eluent, R_f value. Melting point: melting point apparatus SMP 3 (Stuart Scientific) was used, uncorrected. ^{1}H NMR (400 MHz), ^{13}C NMR (100 MHz): Unity Mercury Plus AS 400 NMR spectrometer (Varian); δ in ppm related to tetramethylsilane; coupling constants are given with 0.5 Hz resolution; the assignments of ^{13}C and ^{1}H NMR signals were supported by 2D NMR techniques. The purity of the compounds was determined by high-performance liquid chromatography (HPLC) analysis (details see Supporting Information). Unless otherwise noted, the purity of all test compounds is >95% according to the HPLC method. The purity of some compounds was determined by elemental analysis.

Spiro[[2]benzopyran]-1,1′-cyclohexan-4′-one (3). A solution of hydroxy acetal **2** (102 mg, 0.37 mmol) and *p*-toluenesulfonic acid monohydrate (12 mg, 0.06 mmol) in CH_2Cl_2 (8 mL) was stirred at rt for 6 d. Subsequently, CH_2Cl_2 (10 mL) was added and the mixture was washed with 0.2 M NaOH (10 mL) and H_2O (10 mL). The aqueous layer was re-extracted with CH_2Cl_2 (10 mL). The combined organic layers were dried (K_2CO_3) and concentrated in vacuo, and the residue was purified by fc (⌀ 3 cm, cyclohexane/ethyl acetate = 4/1, 22 cm, 10 mL). R_f: (cyclohexane/ethyl acetate = 4/1, 0.38). Colorless solid, mp 104 °C, yield 78.5 mg (25%). $C_{14}H_{14}O_2$ (214.3). ^{1}H NMR ($CDCl_3$): δ (ppm) = 2.09 ("td", J = 13.8/4.9 Hz, 2H, $(CH_2CH_2)_2C{=}O$), 2.31–2.39 (m, 2H, $(CH_2CH_2)_2C{=}O$), 2.61–2.69 (m, 2H, $(CH_2CH_2)_2C{=}O$), 2.84 ("td", J = 14.4/6.3 Hz, 2H, $(CH_2CH_2)_2C{=}O$), 5.85 (d, J = 5.6 Hz, 1H, ArC*H*CHO), 6.58 (d, J = 5.7 Hz, 1H, ArCHC*H*O), 7.00 (dd, J = 7.2/1.6 Hz, 1H, Ar-H), 7.06 (dd, J = 7.5/1.2 Hz, 1H, Ar-H), 7.18 ("td", J = 7.4/1.6 Hz, 1H, Ar-H), 7.22 ("td", J = 7.3/1.4 Hz, 1H, Ar-H). Purity (HPLC method A): 96.6%, t_R = 19.2 min.

***trans-N*-(Cyclohexylmethyl)spiro[[2]benzopyran-1,1′-cyclohexan]-4′-amine (4a) and *cis-N*-(Cyclohexylmethyl)spiro[[2]benzopyran-1,1′-cyclohexan]-4′-amine (4b).** Under N_2, a mixture of ketone **3** (75 mg, 0.35 mmol), cyclohexylmethylamine (98%, 63 mg, 0.54 mmol), acetic acid (20 μL, 0.45 mmol), $NaBH(OAc)_3$ (95%, 141 mg, 0.63 mmol), and THF (7 mL) was stirred at rt for 3 h. Subsequently, 1 M NaOH (10 mL) was added and the mixture was extracted with CH_2Cl_2 (3 × 20 mL) and with Et_2O (20 mL). The combined organic layers were dried (K_2CO_3) and concentrated in vacuo, and the residue was purified by fc (⌀ 2.5 cm, cyclohexane/ethyl acetate = 19/1 + 0.5% *N,N*-dimethylethanamine, 15 cm, 10 mL). R_f (cyclohexane/ethyl acetate = 19/1 + 0.5% *N,N*-dimethylethanamine, **4a**: R_f = 0.18, **4b**: R_f = 0.05).

4a: Colorless solid, mp 35 °C, yield 31 mg (28%). $C_{21}H_{29}NO$ (311.5). ^{1}H NMR ($CDCl_3$): δ (ppm) = 0.92("qd", J = 11.9/2.9 Hz, 2H, NCH_2(cyclohexyl-*H*)), 1.11–1.32 (m, 4H, NCH_2(cyclohexyl-*H*)), 1.38–1.50 (m, 1H, NCH_2(cyclohexyl-*H*)), 1.55–1.64 (m, 2H, $(CH_2CH_2)_2CHN$), 1.64–1.83 (m, 4H, NCH_2(cyclohexyl-*H*), 1.87–2.04 (m, 6H, $(CH_2CH_2)_2CHN$)), 2.43 (d, J = 6.6 Hz, 2H, NCH_2(cyclohexyl-H)), 2.87 ("quint", J = 3.0 Hz, 1H, 4′-H_e), 5.72 (d, J = 5.7, 1H, OCH=C*H*Ar), 6.49 (d, J = 5.7 Hz, 1H, OC*H*=CHAr), 6.89–6.94 (m, 1H, Ar-H), 7.12–7.17 (m, 3H, Ar-H). A signal for the NH-proton is not seen in the spectrum.

4b: Colorless solid, mp 85 °C, yield 57 mg (52%). $C_{21}H_{29}NO$ (311.5). ^{1}H NMR ($CDCl_3$): δ (ppm) = 0.86–0.96 (m, 2H, NCH_2(cyclohexyl-*H*)), 1.11–1.33 (m, 4H, NCH_2(cyclohexyl-*H*)), 1.40–1.50 (m, 1H, NCH_2(cyclohexyl-*H*)), 1.54–1.87 (m, 10H, NCH_2(cyclohexyl-*H*) (4H), $(CH_2CH_2)_2CHN$ (6H)), 2.28–2.39 (m, 2H, 2′-H_e, 6′-H_e), 2.47–2.57 (m, 1H, 4′-H_a), 2.50 (d, J = 6.7 Hz, 2H, NCH_2(cyclohexyl-H)), 5.75 (d, J = 5.7 Hz, 1H, OCH=C*H*Ar), 6.47 (d, J = 5.6 Hz, 1H, OC*H*=CHAr), 6.92–6.94 (m, 1H, Ar-H), 7.05–7.07 (m, 1H, Ar-H), 7.12–7.19 (m, 2H, Ar-H). A signal for the NH-proton is not seen in the spectrum.

***trans-N*-(Cyclohexylmethyl)-*N*-methylspiro[[2]benzopyran-1,1′-cyclohexan]-4′-amine (5a).** Under N_2, cyclohexylmethylamine **4a** (23.6 mg, 0.08 mmol) was dissolved in CH_2Cl_2 (5 mL). Formalin (37%, stabilized with 10–15% MeOH, 114 μL, 1.50 mmol) and $NaBH(OAc)_3$ (95%, 27 mg, 0.12 mmol) were added and the reaction mixture was stirred at rt for 2 h. Subsequently, H_2O (10 mL) was added and the mixture was extracted with CH_2Cl_2 (3 × 20 mL) and once Et_2O (20 mL). The combined organic layers were dried (K_2CO_3) and concentrated in vacuo, and the residue was purified by fc (⌀ 2 cm, cyclohexane + 0.5% *N,N*-dimethylethanamine, 15 cm, 10 mL). R_f (cyclohexane + 0.5% *N,N*-dimethylethanamine, 0.09, cyclohexane + 1% *N,N*-dimethylethanamine, 0.35). Colorless oil, yield 20 mg (81%). $C_{22}H_{31}NO$ (325.5). ^{1}H NMR ($CDCl_3$): δ (ppm) = 0.79–0.89 (m, 2H, NCH_2(cyclohexyl-*H*)), 1.10–1.31 (m, 4H, NCH_2(cyclohexyl-*H*)), 1.44–1.55 (m, 1H, NCH_2(cyclohexyl-*H*)), 1.63–1.75 (m, 3H, NCH_2(cyclohexyl-*H*) (1H), $(CH_2CH_2)_2CHN$ (2H)), 1.78–1.88 (m, 5H, NCH_2(cyclohexyl-*H*) (3H), $(CH_2CH_2)_2CHN$ (2H)), 1.91–1.99 (m, 2H, $(CH_2CH_2)_2CHN$), 2.03–2.12 (m, 2H, $(CH_2CH_2)_2CHN$), 2.13 (d, J = 7.1 Hz, 2H, NCH_2(cyclohexyl-H)), 2.17 (s, 3H, NCH_3), 2.24 ("quint", J = 3.3 Hz, 1H, 4′-H_e), 5.72 (d, J = 5.6 Hz, 1H, OCH=C*H*Ar), 6.49 (d, J = 5.6 Hz, 1H, OC*H*=CHAr), 6.90–6.94 (m, 1H, Ar-H), 7.11–7.18 (m, 3H, Ar-H).

***cis-N*-(Cyclohexylmethyl)-*N*-methylspiro[[2]benzopyran-1,1′-cyclohexan]-4′-amine (5b).** Under N_2, cyclohexylmethylamine **4b** (42.6 mg, 0.14 mmol) was dissolved in CH_2Cl_2 (5 mL). Formalin (37%, stabilized with 10–15% MeOH, 205 μL, 2.70 mmol), and $NaBH(OAc)_3$ (95%, 48 mg, 0.22 mmol) were added and the reaction mixture was stirred at rt for 2 h. Subsequently, H_2O (10 mL) was added and the mixture was extracted with CH_2Cl_2 (3 × 20 mL) and once with Et_2O (20 mL). The combined organic layers were dried (K_2CO_3) and concentrated in vacuo, and the residue was purified by fc (⌀ 2 cm, cyclohexane + 0.5% *N,N*-dimethylethanamine, 15 cm, 10 mL). R_f (cyclohexane + 0.5% *N,N*-dimethylethanamine, 0.05, cyclohexane + 1% *N,N*-dimethylethanamine, 0.12). Colorless solid, mp 73 °C, yield 40 mg (90%). $C_{22}H_{31}NO$ (325.5). ^{1}H NMR ($CDCl_3$): δ (ppm) = 0.79–0.92 (m, 2H, NCH_2(cyclohexyl-*H*)), 1.11–1.32 (m, 4H, NCH_2(cyclohexyl-*H*)), 1.35–1.47 (m, 1H, NCH_2(cyclohexyl-*H*)), 1.52–1.84 (m, 10H, NCH_2(cyclohexyl-*H*) (4H), $(CH_2CH_2)_2CHN$ (6H)), 2.23–2.27 (m, 2H, $(CH_2CH_2)_2CHN$, 2.30 (s, 3H, NCH_3)), 2.36–2.40 (m, 2H, NCH_2(cyclohexyl-H)), 2.43–2.54 (m, 1H, 4′-H_a), 5.74 (d, J = 5.6 Hz, 1H, OCH=C*H*Ar), 6.51 (d, J = 5.6 Hz, 1H, OC*H*=CHAr), 6.92–6.94 (m, 1H, Ar-H), 7.05–7.09 (m, 1H, Ar-H), 7.12–7.18 (m, 2H, Ar-H).

***trans-N*-(Cyclohexylmethyl)-3-methoxy-3,4-dihydrospiro-[[2]benzopyran-1,1′-cyclohexan]-4′-amine (10a) and *cis-N*-(Cyclohexylmethyl)-3-methoxy-3,4-dihydrospiro[[2]-benzopyran-1,1′-cyclohexan]-4′-amine (10b).** Under N_2, ketone **9** (146 mg, 0.59 mmol) was dissolved in THF (5 mL). Cyclohexylmethylamine (98%, 89 mg, 0.77 mmol), acetic acid (34 μL, 0.60 mmol), and $NaBH(OAc)_3$ (95%, 212 mg, 0.95 mmol) were added and the mixture was stirred at rt for 4 h. Subsequently, 1 M NaOH (15 mL) was added and the mixture was extracted with Et_2O (3 × 15 mL). The combined organic layers were dried (K_2CO_3) and concentrated in vacuo, and the residue was purified by fc (⌀ 4 cm, cyclohexane + 2% *N,N*-dimethylethanamine, 20 cm, 20 mL). R_f (cyclohexane + 2% *N,N*-dimethylethanamine, **10a**: R_f = 0.24, **10b**: R_f = 0.05).

10a: Colorless solid, mp 56 °C, yield 75 mg (37%). $C_{22}H_{33}NO_2$ (343.6). ^{1}H NMR ($CDCl_3$): δ (ppm) = 0.90–1.03 (m, 2H, NCH_2(cyclohexyl-*H*)), 1.13–1.35 (m, 4H, NCH_2(cyclohexyl-*H*)), 1.40–1.53 (m, 1H, NCH_2(cyclohexyl-*H*)), 1.57–1.87 (m, 8H, NCH_2(cyclohexyl-*H*) (4H), $(CH_2CH_2)_2CHN$) (4H)), 1.90–2.12 (m, 3H, $(CH_2CH_2)_2CHN$), 2.25 ("td", J = 13.6/3.9 Hz, 1H, 2′-H_a), 2.45 (d, J = 6.6 Hz, 2H, NCH_2(cyclohexyl-H), 2.86–2.95 (m, 3H, 4′-H_e (1H), $ArCH_2CHOCH_3$ (2H)), 3.57 (s, 3H, OCH_3), 4.85 (dd, J = 6.7/4.2 Hz, 1H, $ArCH_2CHOCH_3$), 7.05–7.10 (m, 1H, Ar-H), 7.12–7.24 (m, 3H, Ar-H). A signal for the NH-proton is not seen in the spectrum.

10b: Colorless solid, mp 95 °C, yield 107 mg (53%). $C_{22}H_{33}NO_2$ (343.6). ^{1}H NMR ($CDCl_3$): δ (ppm) = 0.86–0.98 (m, 2H, NCH_2(cyclohexyl-*H*)), 1.10–1.33 (m, 4H, NCH_2(cyclohexyl-*H*)), 1.42–1.53 (m, 1H, NCH_2(cyclohexyl-*H*)), 1.55–1.99 (m, 11 H, NCH_2(cyclohexyl-*H*) (4H), $(CH_2CH_2)_2CHN$ (7H)), 2.06–2.12 (m, 1H, 2′-H_e), 2.51–2.60 (m, 3H, NCH_2(cyclohexyl-H) (2H), 4′-H_a (1H)), 2.89 (dd, J = 15.5/6.5 Hz, 1H, $ArCH_2CHOCH_3$), 2.94 (dd, J

= 15.6/3.7 Hz, 1H, ArCH_2CHOCH$_3$), 3.56 (s, 3H, OCH_3), 4.85 (dd, J = 6.7/3.9 Hz, 1H, ArCH$_2$CHOCH$_3$), 7.07–7.13 (m, 2H, Ar-H), 7.13–7.22 (m, 2H, Ar-H). A signal for the NH-proton is not seen in the spectrum.

***trans*-*N*-(Cyclohexylmethyl)-3-methoxy-*N*-methyl-3,4-dihydrospiro[2-benzopyran-1,1′-cyclohexan]-4′-amine (11a).** Under N_2, cyclohexylmethylamine **10a** (44 mg, 0.13 mmol) was dissolved in CH_2Cl_2 (2.5 mL). Formalin (37%, stabilized with 10–15% MeOH, 190 μL, 2.55 mmol), and NaBH(OAc)$_3$ (95%, 46 mg, 0.20 mmol) were added and the reaction mixture was stirred at rt for 2 h. Then, H_2O (10 mL) was added and the mixture was extracted with CH_2Cl_2 (3 × 20 mL) and Et_2O (1 × 10 mL). The combined organic layers were dried (K_2CO_3) and concentrated in vacuo, and the residue was purified by fc (⌀ 2 cm, cyclohexane + 0.5% *N*,*N*-dimethylethanamine, 20 cm, 10 mL). R_f (cyclohexane + 0.5% *N*,*N*-dimethylethanamine: 0.09). Pale yellow solid, mp 60 °C, yield 41 mg (90%). $C_{23}H_{35}NO_2$ (357.6). ^{1}H NMR ($CDCl_3$): δ (ppm) = 0.80–0.95 (m, 2H, NCH$_2$(cyclohexyl-*H*)), 1.11–1.34 (m, 4H, NCH$_2$(cyclohexyl-*H*)), 1.50–1.62 (m, 3H, NCH$_2$(cyclohexyl-*H*)), 1.65–1.80 (m, 4H, NCH$_2$(cyclohexyl-*H*) (2H), (CH_2CH$_2$)$_2$CHN (2H)), 1.84–1.90 (m, 3H, (CH$_2$CH_2)$_2$CHN), 1.90–2.08 (m, 2H, (CH$_2$CH_2)$_2$CHN), 2.16 (dd, J = 7.2/1.5 Hz, 2H, NCH_2(cyclohexyl-H)), 2.20–2.33 (m, 5H, NCH_3 (3H), 4′-H$_e$ (1H), 2′-H$_a$ (1H)), 2.89 (dd, J = 15.7/7.0 Hz, 1H, ArCH_2CHOCH$_3$), 2.94 (dd, J = 15.8/4.0 Hz, 1H, ArCH_2CHOCH$_3$), 3.58 (s, 3H, OCH_3), 4.86 (dd, J = 6.6/4.3 Hz, 1H, ArCH$_2$C*H*OCH$_3$), 7.05–7.09 (m, 1H, Ar-H), 7.12–7.24 (m, 3H, Ar-H).

***cis*-*N*-(Cyclohexylmethyl)-3-methoxy-*N*-methyl-3,4-dihydrospiro[2-benzopyran-1,1′-cyclohexan]-4′-amine (11b).** Under N_2, cyclohexylmethylamine **10b** (46 mg, 0.14 mmol) was dissolved in CH_2Cl_2 (2.5 mL). Formalin (37%, stabilized with 10–15% MeOH, 201 μL, 2.70 mmol), and NaBH(OAc)$_3$ (95%, 48 mg, 0.22 mmol) were added and the reaction mixture was stirred at rt for 2 h. Then, H_2O (10 mL) was added and the mixture was extracted with CH_2Cl_2 (3 × 20 mL) and Et_2O (1 × 10 mL). The combined organic layers were dried (K_2CO_3) and concentrated in vacuo, and the residue was purified by fc (⌀ 2 cm, cyclohexane + 1% *N*,*N*-dimethylethanamine, 20 cm, 10 mL). R_f (cyclohexane + 1% *N*,*N*-dimethylethanamine: 0.15). Pale yellow solid, mp 77 °C, yield 43 mg (89%). $C_{23}H_{35}NO_2$ (357.6). ^{1}H NMR ($CDCl_3$): δ (ppm) = 0.79–0.91 (m, 2H, NCH$_2$(cyclohexyl-*H*)), 1.10–1.32 (m, 3H, NCH$_2$(cyclohexyl-*H*)), 1.36–1.49 (m, 1H, NCH$_2$(cyclohexyl-*H*)), 1.57–1.75 (m, 6H, NCH$_2$(cyclohexyl-*H*) (5H), (CH_2CH$_2$)$_2$CHN (1H)), 1.76–1.84 (m, 3H, (CH$_2$CH_2)$_2$CHN), 1.85–2.01 (m, 3H, (CH$_2$CH_2)$_2$CHN), 2.09–2.17 (m, 1H, 2′-H$_e$), 2.25 (d, J = 6.8 Hz, 2H, NCH_2(cyclohexyl-H)), 2.31 (s, 3H, NCH_3), 2.49–2.59 (m, 1H, 4′-H$_a$), 2.89 (dd, J = 15.5/6.5 Hz, 1H, ArCH_2CHOCH$_3$), 2.94 (dd, J = 15.5/3.5 Hz, 1H, ArCH_2CHOCH$_3$), 3.59 (s, 3H, OCH_3), 4.86 (dd, J = 6.9/3.9 Hz, 1H, ArCH$_2$C*H*OCH$_3$), 7.06–7.22 (m, 4H, Ar-H).

3-Methoxy-3*H*-spiro[[2]-benzofuran-1,1′-cyclohexan]-4′-one (13). Under N_2, a solution of 2-bromobenzaldehyde dimethyl acetal (**12**, 257 mg, 1.11 mmol) in THF abs. (12 mL) was cooled to −78 °C. Subsequently, *n*-BuLi (1.6 M in *n*-hexane, 0.84 mL, 1.34 mmol) was added dropwise. After 20 min, cyclohexane-1,4-dione (250 mg, 2.23 mmol in THF abs., 2 mL) was added rapidly and the mixture was stirred at −78 °C for 20 min and 1 h at rt. Then, H_2O was added and the mixture was extracted with Et_2O (2×) and CH_2Cl_2 (2×). The organic layer was concentrated in vacuo and the residue was purified by fc (4 cm, cyclohexane/ethyl acetate = 2/1), 24 cm, 20 mL, R_f (cyclohexane/ethyl acetate = 2/1, 0.21). The isolated product (contaminated, 177 mg) was dissolved in THF, *p*-toluenesulfonic acid monohydrate (23 mg, 0.12 mmol) was added and the mixture was stirred at rt for 24 h. Subsequently, 0.2 M NaOH (20 mL) was added and the aqueous layer was extracted with Et_2O (3 × 20 mL). The combined organic layers were dried (K_2CO_3) and concentrated in vacuo, and the residue was purified by fc (⌀ 4.5 cm, cyclohexane/ethyl acetate = 6/1, 21 cm, 20 mL). R_f (cyclohexane/ethyl acetate = 6/1, 0.20). Colorless solid, mp 129 °C, yield 113 mg (44%). $C_{14}H_{16}O_3$ (232.3). ^{1}H NMR ($CDCl_3$): δ (ppm) = 2.01–2.08 (m, 1H, (CH_2CH$_2$)$_2$C=O), 2.14–2.29 (m, 3H, (CH_2CH$_2$)$_2$C=O), 2.39–2.46 (m, 2H, (CH$_2$CH_2)$_2$C=O), 2.90–3.00 (m, 2H, (CH$_2$CH_2)$_2$C=O), 3.54 (s, 3H, OCH$_3$), 6.16 (s, 1H, ArC*H*OCH$_3$), 7.12–7.17 (m, 1H, Ar-H), 7.35–7.42 (m, 3H, Ar-H).

***trans*-*N*-(Cyclohexylmethyl)-3-methoxy-3*H*-spiro[[2]-benzofuran-1,1′-cyclohexan]-4′-amine (14a) and *cis*-*N*-(Cyclohexylmethyl)-3-methoxy-3*H*-spiro[[2]benzofuran-1,1′-cyclohexan]-4′-amine (14b).** Under N_2, ketone **13** (90 mg, 0.39 mmol) was dissolved in THF (5 mL). Cyclohexylmethylamine (98%, 69 mg, 0.58 mmol) in THF abs. (1 mL), acetic acid (25 μL, 0.44 mmol), and NaBH(OAc)$_3$ (95%, 156 mg, 0.67 mmol) were added, and the mixture was stirred at rt for 3 h. Subsequently, 1 M NaOH (10 mL) was added and the mixture was extracted with CH_2Cl_2 (3 × 20 mL) and Et_2O (20 mL). The combined organic layers were dried (K_2CO_3) and concentrated in vacuo, and the residue was purified by fc (⌀ 3 cm, cyclohexane + 2% *N*,*N*-dimethylethanamine, 20 cm, 10 mL). R_f (cyclohexane + 2% *N*,*N*-dimethylethanamine, **14a**: R_f = 0.20, **14b**: R_f = 0.10).

14a: Colorless oil, yield 36 mg (28%). $C_{21}H_{31}NO_2$ (329.5). ^{1}H NMR ($CDCl_3$): δ (ppm) = 0.94 ("qd", J = 12.0/2.8 Hz, 2H, NCH$_2$(cyclohexyl-*H*)), 1.12–1.33 (m, 4H, NCH$_2$(cyclohexyl-*H*)), 1.41–1.53 (m, 1H, NCH$_2$(cyclohexyl-*H*)), 1.55–1.85 (m, 8H, NCH$_2$(cyclohexyl-*H*) (4H), (CH_2CH$_2$)$_2$CHN) (4H)), 1.93–2.10 (m, 4H, (CH_2CH$_2$)$_2$CHN), 2.47 (d, J = 6.4 Hz, 2H, NCH_2(cyclohexyl-H), 2.80–2.87 (m, 1H, 4′-H$_e$), 3.46 (s, 3H, OCH$_3$), 6.06 (s, 1H, ArC*H*OCH$_3$), 7.29–7.38 (m, 4H, Ar-H). A signal for the NH-proton is not seen in the spectrum.

14b: Colorless oil, yield 86 mg (67%). $C_{21}H_{31}NO_2$ (329.5). ^{1}H NMR ($CDCl_3$): δ (ppm) = 0.85–0.99 (m, 2H, NCH$_2$(cyclohexyl-*H*)), 1.11–1.33 (m, 4H, NCH$_2$(cyclohexyl-*H*)), 1.41–1.52 (m, 1H, NCH$_2$(cyclohexyl-*H*)), 1.60–1.85 (m, 9H, NCH$_2$(cyclohexyl-*H*) (4H), (CH_2CH$_2$)$_2$CHN) (5H)), 1.85–1.97 (m, 3H, (CH$_2$CH_2)$_2$CHN), 2.49–2.61 (m, 1H, 4′-H$_a$), 2.52 (d, J = 7.4 Hz, 2H, NCH_2(cyclohexyl-H), 3.48 (s, 3H, OCH$_3$), 6.04 (s, 1H, ArC*H*OCH$_3$), 7.09–7.13 (m, 1H, Ar-H), 7.28–7.38 (m, 3H, Ar-H). A signal for the NH-proton is not seen in the spectrum.

3,4-Dihydrospiro[[2]benzopyran-1,1′-cyclohexan]-4′-one Ethylene Ketal (17). Under N_2, a solution of 1-bromo-2-(2-bromoethyl)benzene (**16**, 202 mg, 0.77 mmol) in THF (10 mL) was cooled to −88 °C. Subsequently, *n*-BuLi (1.6 M in *n*-hexane, 0.58 mL, 0.93 mmol) was added slowly. After stirring for 5 min at −88 °C, cyclohexane-1,4-dione monoethylene ketal (0.168 g), 1.08 mmol in THF (2 mL) was added rapidly, and the mixture was stirred at −88 °C for 5 min and at rt for additional 1 h. Then, H_2O (10 mL) was added, and the mixture was extracted with Et_2O (3 × 40 mL). The combined organic layers were dried (K_2CO_3) and concentrated in vacuo, and the residue was purified by fc (⌀ 4 cm, cyclohexane/ethyl acetate = 9/1, 20 cm, 20 mL). R_f (cyclohexane/ethyl acetate = 9/1, 0.18). Colorless solid, mp 122 °C, yield 121 mg (61%). $C_{16}H_{20}O_3$ (260.4). ^{1}H NMR ($CDCl_3$): δ (ppm) = 1.60–1.65 (m, 2H, (CH_2CH$_2$)$_2$C=O), 1.94–2.07 (m, 6H, (CH_2CH$_2$)$_2$C=O), 2.83 (t, J = 5.4 Hz, 2H, ArCH_2CH$_2$O), 3.91 (t, J = 5.6 Hz, 2H, ArCH$_2$CH_2O), 4.00 (s, 4H, OCH_2CH_2O), 7.06–7.10 (m, 1H, Ar-H), 7.12–7.16 (m, 1H, Ar-H), 7.16–7.20 (m, 2H, Ar-H).

3,4-Dihydrospiro[[2]benzopyran-1,1′-cyclohexan]-4′-one (18). A solution of ketal **17** (121 mg, 0.47 mmol) in Et_2O (4 mL) and 2 M HCl (4 mL) was heated to reflux for 48 h. Intermediately evaporated Et_2O was supplemented. Subsequently, H_2O (50 mL) and Et_2O (50 mL) were added and the mixture was extracted with Et_2O (3 × 50 mL). The combined organic layers were dried (K_2CO_3) and concentrated in vacuo, and the residue was purified by fc (⌀ 2 cm, cyclohexane/ethyl acetate = 9/1, 20 cm, 10 mL). R_f (cyclohexane/ethyl acetate = 9/1, 0.10, cyclohexane/ethyl acetate = 4/1, 0.23). Colorless solid, mp 134 °C, yield 93.5 mg (94%). $C_{14}H_{16}O_2$ (216.3). ^{1}H NMR ($CDCl_3$): δ (ppm) = 2.18 ("td", J = 13.8/4.6 Hz, 2H, (CH_2CH$_2$)$_2$C=O), 2.26–2.34 (m, 4H, (CH_2CH$_2$)$_2$C=O), 2.86 ("td", J = 14.3/6.3 Hz, 2H, (CH$_2$CH_2)$_2$C=O), 2.90 (t, J = 5.5 Hz, 2H, ArCH_2CH$_2$O), 4.01 (t, J = 5.6 Hz, 2H, ArCH$_2$CH_2O), 7.05–7.10 (m, 1H, Ar-H), 7.11–7.22 (m, 3H, Ar-H).

***trans*-*N*-(Cyclohexylmethyl)-3,4-dihydrospiro[[2]-benzopyran-1,1′-cyclohexan]-4′-amine (19a) and *cis*-*N*-(Cyclohexylmethyl)-3,4-dihydrospiro[[2]benzopyran-1,1′-cyclohexan]-4′-amine (19b).** Under N_2, a solution of ketone **18** (85 mg, 0.39 mmol) in THF (5 mL) was treated with cyclohexylmethylamine (98%, 68 mg, 0.59 mmol) dissolved in THF (2 mL), acetic acid (23 μL, 0.40 mmol), and $NaBH(OAc)_3$ (95%, 158 mg, 0.71 mmol). The mixture was stirred at rt for 3 h. Subsequently, 1 M NaOH (10 mL) was added and the mixture was extracted with CH_2Cl_2 (3 × 20 mL) and Et_2O (20 mL). The combined organic layers were dried (K_2CO_3) and concentrated in vacuo, and the residue was purified by fc (⌀ 3 cm, cyclohexane + 2% *N*,*N*-dimethylethanamine, 20 cm, 10 mL). R_f (cyclohexane + 2% *N*,*N*-dimethylethanamine, **19a**: R_f = 0.33, **19b**: R_f = 0.09).

19a: Colorless oil, yield 30 mg (24%). $C_{21}H_{31}NO$ (313.5). ^1H NMR ($CDCl_3$): δ (ppm) = 0.90−1.00 (m, 2H, NCH_2(cyclohexyl-*H*)), 1.13−1.34 (m, 4H, NCH_2(cyclohexyl-*H*)), 1.43−1.52 (m, 1H, NCH_2(cyclohexyl-*H*)), 1.53−1.62 (m, 2H, $(CH_2CH_2)_2CHN$), 1.62−1.70 (m, 4H, NCH_2(cyclohexyl-*H*) (2H), $(CH_2CH_2)_2CHN$ (2H)), 1.79−1.86 (m, 2H, NCH_2(cyclohexyl-*H*)), 1.90 ("tt", *J* = 13.8/3.4 Hz, 2H, 3′-H_a, 5′-H_a), 2.08 ("td", *J* = 13.7/3.7 Hz, 2H, 2′-H_a, 6′-H_a), 2.44 (d, *J* = 6.6 Hz, 2H, NCH_2(cyclohexyl-H)), 2.82 (t, *J* = 5.6 Hz, 2H, OCH_2CH_2Ar), 2.85−2.90 (m, 1H, 4′-H_e), 3.90 (t, *J* = 5.6 Hz, 2H, OCH_2CH_2Ar), 7.06−7.08 (m, 1H, Ar-H), 7.10−7.14 (m, 1H, Ar-H), 7.18−7.19 (m, 2H, Ar-H). A signal for the NH-proton is not seen in the spectrum.

19b: Colorless oil, yield 89 mg (72%). $C_{21}H_{31}NO$ (313.5). ^1H NMR ($CDCl_3$): δ (ppm) = 0.84−0.98 (m, 2H, NCH_2(cyclohexyl-*H*)), 1.10−1.31 (m, 4H, NCH_2(cyclohexyl-*H*)), 1.41−1.51 (m, 1H, NCH_2(cyclohexyl-*H*)), 1.52−1.62 (m, 2H, NCH_2(cyclohexyl-*H*)), 1.63−1.84 (m, 8H, NCH_2(cyclohexyl-*H*) (2H), $(CH_2CH_2)_2CHN$-(6H)), 1.94−2.03 (m, 2H, 2′-H_e, 6′-H_e), 2.50 (d, *J* = 6.7 Hz, 2H NCH_2(cyclohexyl-H)), 2.50−2.59 (m, 1H, 4′-H_a), 2.82 (t, *J* = 5.5 Hz, 2H, OCH_2CH_2Ar), 3.88 (t, *J* = 5.6 Hz, 2H, OCH_2CH_2Ar), 7.07−7.19 (m, 4H, Ar-H). A signal for the NH-proton is not seen in the spectrum.

***trans*-*N*-Benzyl-3-methoxy-3*H*-spiro[[2]benzofuran-1,1′-cyclohexan]-4′-amine (23a) and *cis*-*N*-Benzyl-3-methoxy-3*H*-spiro[[2]benzofuran-1,1′-cyclohexan]-4′-amine (23b).** Under N_2, a solution of ketone **13** (70.5 mg, 0.30 mmol), benzylamine (37 μL, 0.32 mmol), acetic acid (17 μL, 0.30 mmol), and $NaBH(OAc)_3$ (95%, 98 mg, 0.44 mmol) in THF (5 mL) was stirred at rt for 4 h. Subsequently, 1 M NaOH (10 mL) was added and the mixture was extracted with Et_2O (10 mL) and CH_2Cl_2 (2 × 10 mL). The combined organic layers were dried (K_2CO_3) and concentrated in vacuo, and the residue was purified by fc (⌀ 3.5 cm, cyclohexane + 2% *N*,*N*-dimethylethanamine, 20 cm, 10 mL). R_f (cyclohexane + 2% *N*,*N*-dimethylethanamine, **23a**: R_f = 0.16, **23b**: R_f = 0.09).

23a: Pale yellow oil, yield 35.3 mg (36%). $C_{25}H_{25}NO_2$ (323.5). ^1H NMR ($CDCl_3$): δ (ppm) = 1.55−1.62 (m, 1H, $(CH_2CH_2)_2CHN$), 1.67−1.81 (m, 3H, $(CH_2CH_2)_2CHN$), 1.98−2.17 (m, 4H, $(CH_2CH_2)_2CHN$), 2.97 ("quint", *J* = 3.9 Hz, 1H, 4′-H_e), 3.46 (s, 3H, OCH_3), 3.83 (s, 2H, NCH_2Ar), 6.07 (s, 1H, $ArCHOCH_3$), 7.25−7.29 (m, 1H, Ar-H), 7.29−7.40 (m, 8H, Ar-H). A signal for the NH-proton is not seen in the spectrum.

23b: Pale yellow oil, yield 51.9 mg (53%). $C_{25}H_{25}NO_2$ (323.5). ^1H NMR ($CDCl_3$): δ (ppm) = 1.65−1.85 (m, 5H, $(CH_2CH_2)_2CHN$), 1.87−1.93 (m, 1H, $(CH_2CH_2)_2CHN$), 1.93−2.01 (m, 2H, $(CH_2CH_2)_2CHN$), 2.65 ("tt", *J* = 10.4/3.9 Hz, 1H, 4′-H_a), 3.49 (s, 3H, OCH_3), 3.90 (s, 2H, Ar-CH_2-NH), 6.05 (s, 1H, $ArCHOCH_3$), 7.08−7.12 (m, 1H, Ar-H), 7.24−7.29 (m, 1H, Ar-H), 7.30−7.38 (m, 7H, Ar-H). A signal for the NH-proton is not seen in the spectrum.

■ COMPUTATIONAL PROCEDURES

All simulations were carried out using the Pmemd modules of Amber 16,[61] running on our own CPU/GPU calculation cluster. Molecular graphics images were produced using the UCSF Chimera package (v.1.10).[62] Chimera is developed by the Resource for Biocomputing, Visualization, and Informatics at the University of California, San Francisco (supported by NIGMS P41-GM103311). All other graphs were obtained using GraphPad Prism (v. 6.0).

The optimized membrane-bound 3D structure of the σ_1 receptor was obtained starting from the available protein data bank (PDB) file (5HK1)[5] and following a procedure described in detail in literature.[7,8]

All ligands were subjected to an initial energy minimization, with the convergence criterion set to 10^{-4} kcal/(mol Å). A conformational search was carried out using a well-validated, ad hoc developed combined molecular mechanics (MM)/MDs simulated annealing protocol[39,41−46] using Amber 16. Accordingly, the relaxed structures were subjected to five repeated temperature cycles (from 310 to 1000 K and back) using constant-volume/constant-temperature (*NVT*) MD conditions. At the end of each annealing cycle, the structures were again energy-minimized to converge below 10^{-4} kcal/(mol Å), and only the structures corresponding to the minimum energy were used for further modeling.

The optimized structures of all compounds were then docked into the σ_1 binding pocket using Autodock 4.2.6/Autodock Tools 1.4.6[63] on a win64 platform. The resulting docked conformations were clustered and visualized; then, the structure of each resulting complex characterized by the lowest Autodock interaction energy in the prevailing cluster was selected for further modeling.

Each compound/receptor complex obtained from the docking procedure was further refined in Amber 16 using the quenched MDs (QMD) method as previously described (see, for example,[61,63−67] and reference therein). Next, the best energy configuration of each complex resulting from QMD was subsequently solvated by a cubic box of TIP3P water molecules[64] extending at least 10 Å in each direction from the solute. The system was neutralized and the solution ionic strength was adjusted to the physiological value of 0.15 M by adding the proper amounts of Na^+ and Cl^- ions. Each solvated system was relaxed (500 steps of steepest descent followed by 500 other conjugate-gradient minimization steps) and then gradually heated to the target temperature of 25 °C in intervals of 50 ps of constant volume-constant temperature (*NVT*) MD simulations (Verlet integration method, time step 1.0 fs). The Langevin thermostat was used to control temperature. During this phase of MD, the protein was restrained with a force constant of 2.0 kcal/(mol Å), and all simulations were carried out with periodic boundary conditions. Subsequently, the density of the system was equilibrated via MD runs in the isothermal−isobaric (*NPT*) ensemble, with a time step of 1 fs. All restraints on the protein atoms were then removed, and each system was further equilibrated using *NPT* MD runs at 25 °C. Three equilibration steps were performed (4 ns each, time step 2.0 fs). System stability was monitored by the fluctuations of the root-mean-square-deviation of the simulated position of the backbone atoms of the σ_1 receptor with respect to those of the initial protein model. The equilibration phase was followed by a data production run consisting of 50 ns of MD simulations in the *NVT* ensemble. Data collection was performed on over the last 20 ns of each equilibrated MD trajectory were considered for statistical data collections. One thousand trajectory snapshots were analyzed for each compound/receptor complex.

The free energy of binding ΔG_{comp} and its major components (ΔH_{comp} and $T\Delta S_{comp}$) between the selected compounds and the σ_1 receptor was estimated by resorting to the well-validated MM/Poisson–Boltzmann surface area (MM/PBSA) approach[65] implemented in Amber 16. The per residue binding free-energy decomposition (interaction spectra) was carried out using the MMs/generalized Boltzmann surface area approach[66,67] and was based on the same snapshots used in the binding free-energy calculation.

FLUORESCENCE MEASUREMENTS WITH FURA-2

Concentrations $c(Ca^{2+}_i)$ were measured in single PC12 cells using the fluorescent indicator fura-2-AM in combination with a monochromator-based imaging system (FEI today Thermo Fisher Scientific, SCR_008452) attached to a fluid immersion objective. Cells were loaded with 0.5 μM fura-2-AM and 0.01% Pluronic F-127 for 30 min at 37 °C in a standard solution composed of 138 mM NaCl, 6 mM KCl, 1 mM $MgCl_2$, 2 mM $CaCl_2$, 5.5 mM glucose, and 10 mM HEPES (adjusted to pH 7.4 with NaOH at 37 °C). Cover slips were then washed in fresh buffer for 30 min and mounted in a perfusion chamber on the stage of the microscope (Olympus EX51WI, Hamburg, Germany). For measurements of $c(Ca^{2+}_i)$, cells were excited at 340 and 380 nm and emission was measured at 510 nm. After correction for background fluorescence, the fluorescence ratio F_{340}/F_{380} of the emission was calculated. Fura-2-signals were calibrated according to the method of Grynkiewicz et al.,[68] using a KD value of 224 nM. Ten to twenty cells were measured on slide and at least two replicates/independent experiments were conducted. At least five independent experiments were conducted.

AUTHOR INFORMATION

Corresponding Author

*E-mail: wuensch@uni-muenster.de. Phone: +49-251-8333311. Fax: +49-251-8332144.

ORCID

Carmen Almansa: 0000-0001-5665-4685
Erik Laurini: 0000-0001-6092-6532
Sabrina Pricl: 0000-0001-8380-4474
Bernhard Wünsch: 0000-0002-9030-8417

Notes

The authors declare no competing financial interest.

ACKNOWLEDGMENTS

This work was supported by the Deutsche Forschungsgemeinschaft (DFG) and the Cells-in-motion Cluster of Excellence (EXC, 1300-CiM), University of Münster, Germany.

ABBREVIATIONS

3D, three-dimensional; DOR, δ-opioid receptor; DTG, 1,3-di(*o*-tolyl)guanidine; ER, endoplasmic reticulum; fc, flash column chromatography; KOR, κ-opioid receptor; MD, molecular dynamics; MM/PBSA, molecular mechanics/Poisson–Boltzmann surface area; MOR, μ-opioid receptor; NADPH, nicotinamide adenine dinucleotide; NMDA, *N*-methyl-D-aspartate; PCP, phencyclidine ((1-phenylcyclohexyl)piperidine); PDB, protein data bank; PGRMC-1, Progesterone receptor membrane component 1; QMD, quenched molecular dynamics; *p*-TsOH, *p*-toluenesulfonic acid; SAR, structure–activity relationships; SEM, standard error of the mean; TMEM97, transmembrane protein 97

REFERENCES

(1) Martin, W. R.; Eades, C. G.; Thompson, J. A.; Huppler, R. E.; Gilbert, P. E. The effects of morphine- and nalorphine- like drugs in the nondependent and morphine-dependent chronic spinal dog. *J. Pharmacol. Exp. Ther.* **1976**, *197*, 517–532.

(2) Gilbert, P. E.; Martin, W. R. The effects of morphine and nalorphine-like drugs in the nondependent, morphine-dependent and cyclazocine-dependent chronic spinal dog. *J. Pharmacol. Exp. Ther.* **1976**, *198*, 66–82.

(3) Hellewell, S. B.; Bruce, A.; Feinstein, G.; Orringer, J.; Williams, W.; Bowen, W. D. Rat liver and kidney contain high densities of σ1 and σ2 receptors: characterization by ligand binding and photoaffinity labeling. *Eur. J. Pharmacol.* **1994**, *268*, 9–18.

(4) Quirion, R.; Bowen, W. D.; Itzhak, Y.; Junien, J. L.; Musacchio, J.; Rothman, R. B.; Tsung-Ping, S.; Tam, S. W.; Taylor, D. P. A proposal for the classification of sigma binding sites. *Trends Pharmacol. Sci.* **1992**, *13*, 85–86.

(5) Schmidt, H. R.; Zheng, S.; Gurpinar, E.; Koehl, A.; Manglik, A.; Kruse, A. C. Crystal structure of the human σ_1 receptor. *Nature* **2016**, *532*, 527–530.

(6) Schmidt, H. R.; Betz, R. M.; Dror, R. O.; Kruse, A. C. Structural basis for σ_1 receptor ligand recognition. *Nat. Struct. Mol. Biol.* **2018**, *25*, 981–987.

(7) Laurini, E.; Dal Col, V.; Mamolo, M. G.; Zampieri, D.; Posocco, P.; Fermeglia, M.; Vio, L.; Pricl, S. Homology model and docking-based virtual screening for ligands of the σ_1 receptor. *ACS Med. Chem. Lett.* **2011**, *2*, 834–839.

(8) Brune, S.; Schepmann, D.; Klempnauer, K.-H.; Marson, D.; Dal Col, V.; Laurini, E.; Fermeglia, M.; Wünsch, B.; Pricl, S. The Sigma Enigma: In Vitro/in Silico Site-Directed Mutagenesis Studies Unveil σ1 Receptor Ligand Binding. *Biochemistry* **2014**, *53*, 2993–3003.

(9) Ortega-Roldan, J. L.; Ossa, F.; Amin, N. T.; Schnell, J. R. Solution NMR studies reveal the location of the second transmembrane domain of the human sigma-1 receptor. *FEBS Lett.* **2015**, *589*, 659–665.

(10) Mavlyutov, T. A.; Yang, H.; Epstein, M. L.; Ruoho, A. E.; Yang, J.; Guo, L.-W. APEX2-enhanced electron microscopy distinguishes sigma-1 receptor localization in the nucleoplasmic reticulum. *Oncotarget* **2018**, *31*, 51317–51330.

(11) Lupardus, P. J.; Wilke, R. A.; Aydar, E.; Palmer, C. P.; Chen, Y.; Ruoho, A. E.; Jackson, M. B. Membrane-delimited coupling between sigma receptors and K^+ channels in rat neurohypophysial terminals requires neither G-Protein nor ATP. *J. Physiol.* **2000**, *526*, 527–539.

(12) Hong, W.; Werling, L. L. Evidence that the σ_1 receptor is not directly coupled to G proteins. *Eur. J. Pharmacol.* **2000**, *408*, 117−125.
(13) Hayashi, T.; Su, T.-P. Sigma-1 Receptor Chaperones at the ER- Mitochondrion Interface Regulate Ca2+ Signaling and Cell Survival. *Cell* **2007**, *131*, 596−610.
(14) Hong, W. C.; Yano, H.; Hiranita, T.; Chin, F. T.; McCurdy, C. R.; Su, T.-P.; Amara, S. G.; Katz, J. L. The sigma-1 receptor modulates dopamine transporter conformation and cocaine binding and may thereby potentiate cocaine self-administration in rats. *J. Biol. Chem.* **2017**, *292*, 11250−11261.
(15) Hascoet, M.; Bourin, M.; Payeur, R.; Lombet, A.; Peglion, J. L. Sigma ligand S14905 and locomotor activity in mice. *Eur. Neuropsychopharmacol.* **1995**, *5*, 481−489.
(16) Matsumoto, R. R.; McCracken, K. A.; Pouw, B.; Miller, J.; Bowen, W. D.; Williams, W.; De Costa, B. R. N-alkyl substituted analogs of the sigma receptor ligand BD1008 and traditional sigma receptor ligands affect cocaine-induced convulsions and lethality in mice. *Eur. J. Pharmacol.* **2011**, *411*, 261−273.
(17) Sharkey, J.; Glen, K. A.; Wolfe, S.; Kuhar, M. J. Cocaine binding at σ receptors. *Eur. J. Pharmacol.* **1988**, *149*, 171−174.
(18) Robson, M. J.; Turner, R. C.; Naser, Z. J.; McCurdy, C. R.; Huber, J. D.; Matsumoto, R. R. SN79, a sigma receptor ligand, blocks methamphetamine-induced microglial activation and cytokine upregulation. *Exp. Neurol.* **2013**, *247*, 134−142.
(19) Díaz, J. L.; Cuberes, R.; Berrocal, J.; Contijoch, M.; Christmann, U.; Fernandez, A.; Port, A.; Holenz, J.; Buschmann, H.; Laggner, C.; Serafini, M. T.; Burgueño, J.; Zamanillo, D.; Merlos, M.; Vela, J. M.; Almansa, C. Synthesis and Biological Evaluation of the 1-Arylpyrazole Class of σ1 Receptor Antagonists: Identification of 4-{2-[5-Methyl-1-(naphthalen-2-yl)-1H-pyrazol-3-yloxy]ethyl}-morpholine (S1RA, E-52862). *J. Med. Chem.* **2012**, *55*, 8211−8224.
(20) Wünsch, B. The σ_1 receptor antagonist S1RA Is a promising candidate for the treatment of neurogenic pain. *J. Med. Chem.* **2012**, *55*, 8209−8210.
(21) Vilner, B. J.; John, C. S.; Bowen, W. D. Sigma-1 and sigma-2 receptors are expressed in a wide variety of human and rodent tumor cell lines. *Cancer Res.* **1995**, *55*, 408−413.
(22) Hashimoto, K.; Ishiwata, K. Sigma receptor ligands: possible application as therapeutic drugs and radiopharmaceuticals. *Curr. Pharm. Des.* **2006**, *12*, 3857−3876.
(23) Collina, S.; Bignardi, E.; Rui, M.; Rossi, D.; Gaggeri, R.; Zamagni, A.; Cortesi, M.; Tesei, A. Are sigma modulators an effective opportunity for cancer treatment? A patent overview (1996-2016). *Expert Opin. Ther. Pat.* **2017**, *27*, 565−578.
(24) Ahmed, I. S.; Rohe, H. J.; Twist, K. E.; Mattingly, M. N.; Craven, R. J. Progesterone receptor membrane component 1 (Pgrmc1): a heme-1 domain protein that promotes tumorigenesis and is inhibited by a small molecule. *J. Pharmacol. Exp. Ther.* **2010**, *333*, 564−573.
(25) Alon, A.; Schmidt, H. R.; Wood, M. D.; Sahn, J. J.; Martin, S. F.; Kruse, A. C. Identification of the gene that codes for the σ2receptor. *Proc. Natl. Acad. Sci. U.S.A.* **2017**, *114*, 7160−7165.
(26) Mach, R. H.; Zeng, C.; Hawkins, W. G. The sigma-2 (σ_2) receptor: a novel protein for the imaging and treatment of cancer. *J. Med. Chem.* **2013**, *56*, 7137−7160.
(27) Mach, R. H.; Wheeler, K. T. Imaging the proliferative status of tumors with PET. *J. Labelled Compd. Radiopharm.* **2007**, *50*, 366−369.
(28) Mach, R. H.; Smith, C. R.; al-Nabulsi, I.; Whirrett, B. R.; Childers, S. R.; Wheeler, K. T. Sigma 2 receptors as potential biomarkers of proliferation in breast cancer. *Cancer Res.* **1997**, *57*, 156−161.
(29) Maier, C. A.; Wünsch, B. Novel Spiropiperidines as Highly Potent and Subtype Selective σ-Receptor Ligands. Part 1. *J. Med. Chem.* **2002**, *45*, 438−448.
(30) Maier, C. A.; Wünsch, B. Novel σ Receptor Ligands. Part 2. SAR of Spiro[[2]benzopyran-1,4'-piperidines] and Spiro[[2]-benzofuran-1,4'-piperidines] with Carbon Substituents in Position 3. *J. Med. Chem.* **2002**, *45*, 4923−4930.
(31) Rack, E.; Fröhlich, R.; Schepmann, D.; Wünsch, B. Design, synthesis and pharmacological evaluation of spirocyclic σ1 receptor ligands with exocyclic amino moiety (increased distance 1). *Bioorg. Med. Chem.* **2011**, *19*, 3141−3151.
(32) Wünsch, B. Eine neue Methode zur Darstellung von 3-Alkoxy- und 3-Hydroxy-3,4-dihydro-1H-2-benzopyranen. *Arch. Pharm.* **1990**, *323*, 493−499.
(33) Abdel-Magid, A. F.; Mehrman, S. J. A Review on the use of sodium triacetoxyborohydride in the reductive amination of ketones and aldehydes. *Org. Process Res. Dev.* **2006**, *10*, 971−1031.
(34) Parham, W. E.; Jones, L. D.; Sayed, Y. A. Selective halogen-lithium exchange in bromophenylalkyl halides. *J. Org. Chem.* **1976**, *41*, 1184−1186.
(35) Hasebein, P.; Frehland, B.; Lehmkuhl, K.; Fröhlich, R.; Schepmann, D.; Wünsch, B. Synthesis and pharmacological evaluation of like- and unlike-configured tetrahydro-2-benzazepines with the α-substituted benzyl moiety in the 5-position. *Org. Biomol. Chem.* **2014**, *12*, 5407−5426.
(36) Meyer, C.; Neue, B.; Schepmann, D.; Yanagisawa, S.; Yamaguchi, J.; Würthwein, E.-U.; Itami, K.; Wünsch, B. Improvement of σ1 receptor affinity by late-stage C-H-bond arylation of spirocyclic lactones. *Bioorg. Med. Chem.* **2013**, *21*, 1844−1856.
(37) Miyata, K.; Schepmann, D.; Wünsch, B. Synthesis and σ receptor affinity of regioisomeric spirocyclic furopyridines. *Eur. J. Med. Chem.* **2014**, *83*, 709−716.
(38) Brune, S.; Schepmann, D.; Lehmkuhl, K.; Frehland, B.; Wünsch, B. Characterization of ligand binding to the σ_1 receptor in a human tumor cell line (RPMI 8226) and establishment of a competitive receptor binding assay. *Assay Drug Dev. Technol.* **2012**, *10*, 365−374.
(39) Weber, F.; Brune, S.; Börgel, F.; Lange, C.; Korpis, K.; Bednarski, P. J.; Laurini, E.; Fermeglia, M.; Pricl, S.; Schepmann, D.; Wünsch, B. Rigidity versus flexibility: is this an Issue in σ_1 receptor ligand affinity and activity? *J. Med. Chem.* **2016**, *59*, 5505−5519.
(40) Schepmann, D.; Lehmkuhl, K.; Brune, S.; Wünsch, B. Expression of σ receptors of human urinary bladder tumor cells (RT-4 cells) and development of a competitive receptor binding assay for the determination of ligand affinity to human σ2 receptors. *J. Pharm. Biomed. Anal.* **2011**, *55*, 1136−1141.
(41) Kokornaczyk, A. K.; Schepmann, D.; Yamaguchi, J.; Itami, K.; Laurini, E.; Fermeglia, M.; Pricl, S.; Wünsch, B. Thiazole-based σ_1 receptor ligands: diversity by late-stage C-H arylation of thiazoles, structure-affinity and selectivity relationships, and molecular interactions. *ChemMedChem* **2017**, *12*, 1070−1080.
(42) Weber, F.; Brune, S.; Korpis, K.; Bednarski, P. J.; Laurini, E.; Dal Col, V.; Pricl, S.; Schepmann, D.; Wünsch, B. Synthesis, pharmacological evaluation, and σ_1 receptor interaction analysis of hydroxyethyl substituted piperazines. *J. Med. Chem.* **2014**, *57*, 2884−2894.
(43) Zampieri, D.; Laurini, E.; Vio, L.; Fermeglia, M.; Pricl, S.; Wünsch, B.; Schepmann, D.; Mamolo, M. G. Improving selectivity preserving affinity: new piperidine-4-carboxamide derivatives as effective sigma-1-ligands. *Eur. J. Med. Chem.* **2015**, *90*, 797−808.
(44) Laurini, E.; Da Col, V.; Wünsch, B.; Pricl, S. Analysis of the molecular interactions of the potent analgesic S1RA with the σ_1 receptor. *Bioorg. Med. Chem. Lett.* **2013**, *23*, 2868−2871.
(45) Laurini, E.; Marson, D.; Dal Col, V.; Fermeglia, M.; Mamolo, M. G.; Zampieri, D.; Vio, L.; Pricl, S. Another brick in the wall. Validation of the σ_1 receptor 3D model by computer-assisted design, synthesis, and activity of new σ_1 ligands. *Mol. Pharm.* **2012**, *9*, 3107−3126.
(46) Meyer, C.; Schepmann, D.; Yanagisawa, S.; Yamaguchi, J.; Dal Col, V.; Laurini, E.; Itami, K.; Pricl, S.; Wünsch, B. Pd-catalyzed direct C-H bond functionalization of spirocyclic σ_1 ligands: generation of a pharmacophore model and analysis of the reverse binding mode by docking into a 3D homology model of the σ_1 Receptor. *J. Med. Chem.* **2012**, *55*, 8047−8065.

(47) Tchedre, K. T.; Huang, R.-Q.; Dibas, A.; Krishnamoorthy, R. R.; Dillon, G. H.; Yorio, T. Sigma-1 receptor regulation of voltage-gated calcium channels involves a direct interaction. *Invest. Ophthalmol. Visual Sci.* **2008**, *49*, 4993−5002.
(48) Rao, T.; Cler, J.; Mick, S.; Ragan, D.; Lanthorn, T.; Contreras, P.; Iyengar, S.; Wood, P. Opipramol, a potent sigma ligand, is an anti-Ischemic agent: Neurochemical evidence for an interaction with the *N*-Methyl-D-Aspartate receptor complex *in vivo* by cerebellar cGMP Measurements. *Neuropharmacology* **1990**, *29*, 1199−1204.
(49) Müller, W.; Siebert, B.; Holoubek, G.; Gentsch, C. Neuropharmacology of the anxiolytic drug opripramol, a sigma site ligand. *Pharmacopsychiatry* **2004**, *37*, 189−197.
(50) Wittig, C.; Schepmann, D.; Soeberdt, M.; Daniliuc, C. G.; Wünsch, B. Stereoselective synthesis of conformationally restricted KOR agonists based on the 2,5-diazabicyclo[2.2.2]octane scaffold. *Org. Biomol. Chem.* **2017**, *15*, 6520−6540.
(51) Geiger, C.; Zelenka, C.; Lehmkuhl, K.; Schepmann, D.; Englberger, W.; Wünsch, B. Conformationally Constrained κ Receptor Agonists: Stereoselective Synthesis and Pharmacological Evaluation of 6,8-Diazabicyclo[3.2.2]nonane Derivatives. *J. Med. Chem.* **2010**, *53*, 4212−4222.
(52) Kracht, D.; Rack, E.; Schepmann, D.; Fröhlich, R.; Wünsch, B. Stereoselective synthesis and structure-affinity relationships of bicyclic κ receptoragonists. *Org. Biomol. Chem.* **2010**, *8*, 212−225.
(53) Radesca, L.; Bowen, W. D.; Di Paolo, L.; de Costa, B. R. Synthesis and receptor binding of enantiomeric N-substituted cis-N-[2-(3,4-dichlorophenyl)ethyl]-2-(1-pyrrolidinyl)cyclohexylamines as high-affinity .sigma. receptor ligands. *J. Med. Chem.* **1991**, *34*, 3058−3065.
(54) De Costa, B. R.; Bowen, W. D.; Hellewell, S. B.; George, C.; Rothman, R. B.; Reid, A. A.; Walker, J. M.; Jacobson, A. E.; Rice, K. C. Alterations in the stereochemistry of the kappa-selective opioid agonist U50,488 result in high-affinity sigma ligands. *J. Med. Chem.* **1889**, *32*, 1996−2002.
(55) Caroll, F. I.; Abraham, P.; Parham, K.; Bai, X.; Zhang, X.; Brine, G. A.; Mascarella, S. W.; Martin, B. R.; May, E. L.; Sauss, C.; Di Paolo, L.; Wallace, P.; Walker, J. M.; Bowen, W. D. Enantiomeric N-substituted N-normetazocines: a comparative study of affinities at σ, PCP, and μ opioid receptors. *J. Med. Chem.* **1992**, *35*, 2812−2818.
(56) May, E. L.; Aceto, M. D.; Bowman, E. R.; Bentley, C.; Martin, B. R.; Harris, L. S.; Medzihradsky, F.; Mattson, M. V.; Jacobson, A. E. Antipodal .alpha.-N-(Methyl through Decyl)-N-normetazocines (5,9.alpha.-Dimethyl-2'-hydroxy-6,7-benzomorphans): In vitro and In vivo Properties. *J. Med. Chem.* **1994**, *37*, 3408−3418.
(57) Köhler, J.; Bergander, K.; Fabian, J.; Schepmann, D.; Wünsch, B. Enantiomerically Pure 1,3-Dioxanes as Highly Selective NMDA and σ1 Receptor Ligands. *J. Med. Chem.* **2012**, *55*, 8953−8957.
(58) Banerjee, A.; Schepmann, D.; Köhler, J.; Würthwein, E.-U.; Wünsch, B. Synthesis and SAR studies of chiral non-racemic dexoxadrol analogues as uncompetitive NMDA receptor antagonists. *Bioorg. Med. Chem.* **2010**, *18*, 7855−7867.
(59) Bergkemper, M.; Kronenberg, E.; Thum, S.; Börgel, F.; Daniliuc, C.; Schepmann, D.; Nieto, F. R.; Brust, P.; Reinoso, R. F.; Alvarez, I.; Wünsch, B. Synthesis, Receptor Affinity, and Anti-allodynic Activity of Spirocyclic σ Receptor Ligands with Exocyclic Amino Moiety. *J. Med. Chem.* **2018**, *61*, 9666−9690.
(60) Stresser, D. M. High-throughput screening of human cytochrome P450 inhibitors using eluorometric substrates. methodology for 25 enzyme/substrate pairs. In *Optimization in Drug Discovery: In Vitro Methods*; Yan, Z., Caldwell, G. W., Eds.; Humana Press: Totowa, NJ 2004, pp 215−230.
(61) Case, D. A.; Betz, R. M.; Botello-Smith, W.; Cerutti, D. S.; Cheatham, T. E. I.; Darden, T. A.; Duke, R. E.; Giese, T. J.; Gohlke, H.; Goetz, A. W.; Homeyer, N.; Izadi, S.; Janowski, P.; Kaus, J.; Kovalenko, A.; Lee, T. S.; LeGrand, S.; Li, P.; Lin, C.; Luchko, T.; Luo, R.; Madej, B.; Mermelstein, D.; Merz, K. M.; Monard, G.; Nguyen, H.; Nguyen, H. T.; Omelyan, I.; Onufriev, A.; Roe, D. R.; Roitberg, A.; Sagui, C.; Simmerling, C. L.; Swails, J.; Walker, R. C.; Wang, J.; Wolf, R. M.; Wu, X.; Xiao, L.; York, D. M.; Kollman, P. A. *AMBER*; University of California: San Francisco (CA, USA), 2016.
(62) Pettersen, E. F.; Goddard, T. D.; Huang, C. C.; Couch, G. S.; Greenblatt, D. M.; Meng, E. C.; Ferrin, T. E. UCSF Chimera?A visualization system for exploratory research and analysis. *J. Comput. Chem.* **2004**, *25*, 1605−1612.
(63) Morris, G. M.; Huey, R.; Lindstrom, W.; Sanner, M. F.; Belew, R. K.; Goodsell, D. S.; Olson, A. J. AutoDock4 and AutoDockTools4: automated docking with selective receptor flexibility. *J. Comput. Chem.* **2009**, *30*, 2785−2791.
(64) Jorgensen, W. L.; Chandrasekhar, J.; Madura, J. D.; Impey, R. W.; Klein, M. L. Comparison of simple potential functions for simulating liquid water. *J. Chem. Phys.* **1983**, *79*, 926−935.
(65) Massova, I.; Kollman, P. A. Combined molecular mechanical and continuum solvent approach (MM-PBSA/GBSA) to predict ligand binding. *Perspect. Drug Discovery Des.* **2000**, *18*, 113−135.
(66) Tsui, V.; Case, D. A. Theory and applications of the generalized Born solvation model in macromolecular simulations. *Biopolymers* **2000**, *56*, 275−291.
(67) Onufriev, A.; Bashford, D.; Case, D. A. Modification of the generalized born model suitable for macromolecules. *J. Phys. Chem. B.* **2000**, *104*, 3712−3720.
(68) Grynkiewicz, G.; Poenie, M.; Tsien, R. Y. A new generation of Ca^{2+} indicators with greatly improved fluorescence properties. *J. Biol. Chem.* **1985**, *260*, 3440−3450.